

Spring 5-18-2012

Numerical Modeling of Lifting Flows in the Presence of a Free Surface

Leonardo R. Carmona Vasquez
lcarmona@uno.edu

Follow this and additional works at: <https://scholarworks.uno.edu/td>



Part of the [Ocean Engineering Commons](#)

Recommended Citation

Carmona Vasquez, Leonardo R., "Numerical Modeling of Lifting Flows in the Presence of a Free Surface" (2012). *University of New Orleans Theses and Dissertations*. 1426.
<https://scholarworks.uno.edu/td/1426>

This Thesis is protected by copyright and/or related rights. It has been brought to you by ScholarWorks@UNO with permission from the rights-holder(s). You are free to use this Thesis in any way that is permitted by the copyright and related rights legislation that applies to your use. For other uses you need to obtain permission from the rights-holder(s) directly, unless additional rights are indicated by a Creative Commons license in the record and/or on the work itself.

This Thesis has been accepted for inclusion in University of New Orleans Theses and Dissertations by an authorized administrator of ScholarWorks@UNO. For more information, please contact scholarworks@uno.edu.

Numerical Modelling of Lifting Flows in the Presence of a Free Surface

A Thesis

Submitted to the Graduate Faculty of
The University of New Orleans
in partial fulfilment of the
requirements for the degree of

Master of Science
in
Engineering
Naval Architecture and Marine Engineering

by
Leonardo R. Carmona Vasquez
B.S. Mechanical Engineering, Univeridad Tecnológica de Bolívar (2004)

May 2012

Copyright 2012, Leonardo Carmona

Acknowledgements

I would like to thank Dr. Lothar Birk, who in addition to act as my advisor for this thesis work, gave me the opportunity to work for him as a Research Assistant. Thanks to the support given to me by Dr. Birk, and the School of Naval Architecture and Marine Engineering at the University of New Orleans, I was able to complete my graduate studies.

I would also like to specially thank the faculty committee members for this thesis work: Dr. Brandon Taravella, and Dr. Martin J. Guillot.

I would like to express my gratitude to Professor Christopher McKesson, and again Dr. Brandon Taravella, who provided me with valuable insight, and orientation, when discussing the physics of the lifting flow problem.

My deepest appreciation goes to the faculty and staff of the School of Naval Architecture and Marine Engineering for their contribution to our education: Dr. Pingsha Dong; Mr. George R. Morrissey, Facilities Director; and Dr. William S. Vorus , Professor emeritus.

I would like to thank my family for their unconditional support. My wife Katiana who stayed with me at all times. My mother Clara, who was always interested in the progress of my graduate studies, despite being in a foreign country. My father Orlando, for teaching me how to think positively. My uncle Edgardo, my cosign Victor, and my wife's family for their help.

Contents

List of Figures	vi
Abstract	ix
1 Introduction	1
2 Review of Literature and Theoretical Background	3
2.1 Concepts of Angular Velocity, Vorticity, and Circulation	3
2.1.1 Vorticity	5
2.1.2 Circulation	5
2.1.3 Rate of Change of vorticity	8
2.1.4 Kelvin's Theorem: Rate of change of Circulation	10
2.1.5 Vortex Quantities	12
2.1.6 Two Dimensional Vortex	16
2.1.7 The Biot - Savart Law	21
2.1.8 The Velocity Induced by a straight vortex Segment	22
2.2 Equations and Solution for Incompressible Potential Flow	26
2.2.1 Potential Flows	27
2.2.2 The Laplace Equation	29
2.2.3 Solving the Hydrodynamics Problem Using Potential Flow Theory	30
2.2.4 General Solution of the Incompressible potential flow problem based in Green's Theorem	31

2.2.5	Solution of the Boundary Value Problem for the Flow Around a Fully Submerged Body	37
3	Computational Implementation of Flows with Free Surface	40
3.1	Basic Integral Equation to Describe the Problem	40
3.2	Discretization of Basic Integral Equation	43
3.3	Building the Numerical Solution	46
3.3.1	Exact formulas	47
3.4	Solving the Discretized Integral Equation	56
3.4.1	The Method by Hess and Smith	57
4	Results and Conclusions	59
4.1	Deeply submerged Foil	59
4.2	Submerged Foil Close to the Free Surface	68
4.3	The Free Surface Piercing Foil	72

List of Figures

- 2.1 Angular velocity of a rectangular fluid element 4
- 2.2 Circulation definition. Relation between line integral and surface integral 6
- 2.3 Flow field with circulation (a) and without circulation (b) 7
- 2.4 Circulation produced by a foil after it starts moving 12
- 2.5 vortex line 13
- 2.6 Vortex tube 14
- 2.7 Two dimensional vortex produced by a rotating cylindrical core 17
- 2.8 Velocity induced by a straight vortex segment 23
- 2.9 View angles for velocity induced by a straight vortex segment 24

- 3.1 Foil geometry discretization NACA2415 43
- 3.2 NACA2415 Foil geometry discretization with free surface. Foil Submerged 0.5 chord lengths 44

- 4.1 Foil geometry discretization NACA2415 60
- 4.2 Pressure coefficient c_p . NACA2415 deeply submerged, angle of attack 6 deg. Froude number $Fn = 0.7$ 61
- 4.3 Pressure coefficient c_p . NACA2415 deeply submerged, angle of attack 6 deg. Froude number $Fn = 0.7$ 61
- 4.4 Velocity Distribution $(V/V_\infty)^2$. NACA2415 deeply submerged, angle of attack 6 deg. Froude number $Fn = 0.7$. Result comparison between program XFOIL by Selig (validated experimentally), and the lifting program HL produced as part of this thesis 62

4.5	Result comparison for velocity distribution $(V/V_\infty)^2$ on foil upper surface, between program XFOIL by Selig (validated experimentally), and the lifting program HL produced as part of this thesis. NACA2415 deeply submerged, angle of attack 6 deg. Froude number $Fn = 0.7$	63
4.6	Pressure coefficient c_p . NACA0012 deeply submerged, zero angle of attack.	64
4.7	Velocity Distribution $(V/V_\infty)^2$. NACA0012 deeply submerged, zero angle of attack. Discretization effect comparison, and Froude number effect	64
4.8	Pressure coefficient. NACA0012 deeply submerged. Aspect ratio 4. Angle of attack 6 degrees . 20 foil panels chord-wise. 120 wake panels in the longitudinal direction	65
4.9	Velocity Distribution $(V/V_\infty)^2$. NACA0012 deeply submerged, zero angle of attack no lifting foil vs. lifting case with foil at a 6 degrees angle of attack. Foil discretization 20 panels chord-wise. Froude number $Fn = 0.7$	66
4.10	Velocity Distribution $(V/V_\infty)^2$. NACA0012 deeply submerged, Foil at 6 Degrees angle of attack. Effect of foil discretization 10 panels chord-wise (dotted lines) vs. 25 panels chord-wise (continuous lines). On both cases the Froude number $Fn = 0.7$, and aspect ration 4	66
4.11	Velocity Distribution $(V/V_\infty)^2$. NACA0012 deeply submerged, Foil at 6 Degrees angle of attack. Foil aspect ratio effect on the pressure distribution. Aspect ratio 4 (dot and dash lines) vs. aspect ratio 8 (purple and green continuous lines). vs. aspect ratio 10 (orange and blue continuous lines) vs. aspect ratio 20 (dashed lines. Froude number $Fn = 0.7$	67
4.12	Pressure coefficient. NACA0012 Submerged at 0.5 Chord length. Aspect ratio 4. Angle of attack 6 degrees	68
4.13	Pressure coefficient. NACA0012 Submerged at 0.5 Chord length. Aspect ratio 4. Angle of attack 6 degrees	69
4.14	Wave Elevation. NACA0012 submerged at 0.5 Chord length. Aspect ratio 4. Angle of attack 6 degrees. Froude number 0.5	69
4.15	Pressure coefficient. NACA0012 submerged at 0.5 Chord length. Aspect ratio 4. Angle of attack 6 degrees. Froude number 0.5	71
4.16	Pressure coefficient. NACA0012 Surface piercing foil. Zero angle of attack. No lift. Froude number 0.3.	72
4.17	Wave elevation. NACA0012 Surface piercing foil. Zero angle of attack. No lift. Froude number 0.3.	73

4.18	Wave elevation. NACA0012 Surface piercing foil. Angle of attack 6 degrees. Froude number 0.3.	73
4.19	Wave elevation. NACA0012 Surface piercing foil. Angle of attack 6 degrees. Froude number 0.3.	74

Abstract

This thesis work started as an attempt to create a computational tool to model hydrodynamics problems involving lifting flows. The method employed to solve the problem is potential flow theory.

Despite the fast evolution of computers and the latest developments in Navier-Stokes solvers, such as the Rans methods; potential flow theory offers the possibility to create or use existing computational tools, which allow us modeling hydrodynamics problems in a simpler manner. Navier-Stokes solver can be very expensive from the computational point of view, and require a high level of expertise in order to achieve reliable models.

Based on the above, we have developed a lifting flow modeling tool that we hope can serve as the starting point of a more elaborated method, and a valuable alternative, for the solution of different hydrodynamics problems.

Key words highlighting important concepts related to this thesis work are: Vortex, circulation, potential flow, panel methods, Sources, doublets.

Chapter 1

Introduction

Back in the Spring semester of 2010, the graduate level course *NAME 6160 'Numerical Methods in Hydrodynamics'*, was offered by Dr. Lothar Birk, at the School of Naval Architecture and Marine Engineering at the University of New Orleans. The course went through all the mathematical theory supporting the study of hydrodynamics. Starting with the derivation of the Navier-Stokes' equations; the basics of potential flow theory; the boundary element method; and finally, a full 3D panel method code was assembled for free surface flows, using a linear free surface boundary condition.

All the graduate students that participated in this course were highly amazed with the way the free surface flow problem was modeled, specifically the wave resistance problem. Basically, using a rational mechanics approach, a very complex problem started to appear more simple.

In our numerical methods course we used Fortran as programming language. We modeled the thickness problem using sources, which basically account for symmetric bodies deeply submerged. Using source singularities we can also model free surface flows, consisting on symmetric hulls displacing with constant speed on the free surface.

In the final stage of the mentioned course we modeled a full 3D free surface problem, consisting on a wigley hull advancing with a constant speed through the free surface.

After we finished the numerical methods course, Dr. Birk let us know for who ever was interested, that there were different topics available for our master's degree projects. Among the available subjects there was the lifting flow simulation.

In the current thesis we are creating a computational tool to solve the lifting problem using the potential flow panel method. In chapter 2, we will start by defining the basic concepts related to the lifting problem, such as vorticity, and circulation. This chapter has a dense mathematical content that will help us understand the physics governing the problem.

In chapter 3, we specifically address how to build a computational method to solve lifting

problems, based on the equations derived in chapter 2.

Finally in chapter 4, we will show the results we obtained with the computational tool we developed as part as this research effort. We also propose alternatives to improve the program based on the results obtained, and stablish the preamble of further developments of the computer program.

Chapter 2

Review of Literature and Theoretical Background

2.1 Concepts of Angular Velocity, Vorticity, and Circulation

Consider a control volume, in this case the infinitesimal rectangular fluid element of figure 2.1. The fluid element can rotate, translate and deform. On the right hand side we observe that the fluid element has deformed due to the difference in velocity of the different edges. We notice that the rotation in the edges (1-4) and (2-3) is caused by the difference in horizontal velocity between the edges (1-2) and (4-3). Similarly, the rotation in the edges (1-2) and (3-4) is produced by the difference in vertical velocity between the edges (1-4) and (2-3). Based on this observation we can find the rotational velocity of the fluid element edges as follows:

$$\text{Angular velocity of segment 1-2} = \underline{w}_{1-2} = \frac{\text{relative velocity between pt1 and pt2}}{\text{radius}} \quad (2.1)$$

$$\underline{w}_{1-2} = \frac{\left(v + \frac{\partial v}{\partial x} \Delta x\right) - v}{\Delta x} = \frac{\partial v}{\partial x} \quad (2.2)$$

Similarly, the angular velocity of of the segments (1-4) and (2-3) is

$$\underline{w}_{1-4} = - \frac{u + \frac{\partial u}{\partial y} \Delta y - u}{\Delta y} = - \frac{\partial u}{\partial y} \quad (2.3)$$

As a result of the above analysis we state that the total angular velocity of the fluid element is the average velocity of the two components derived above:

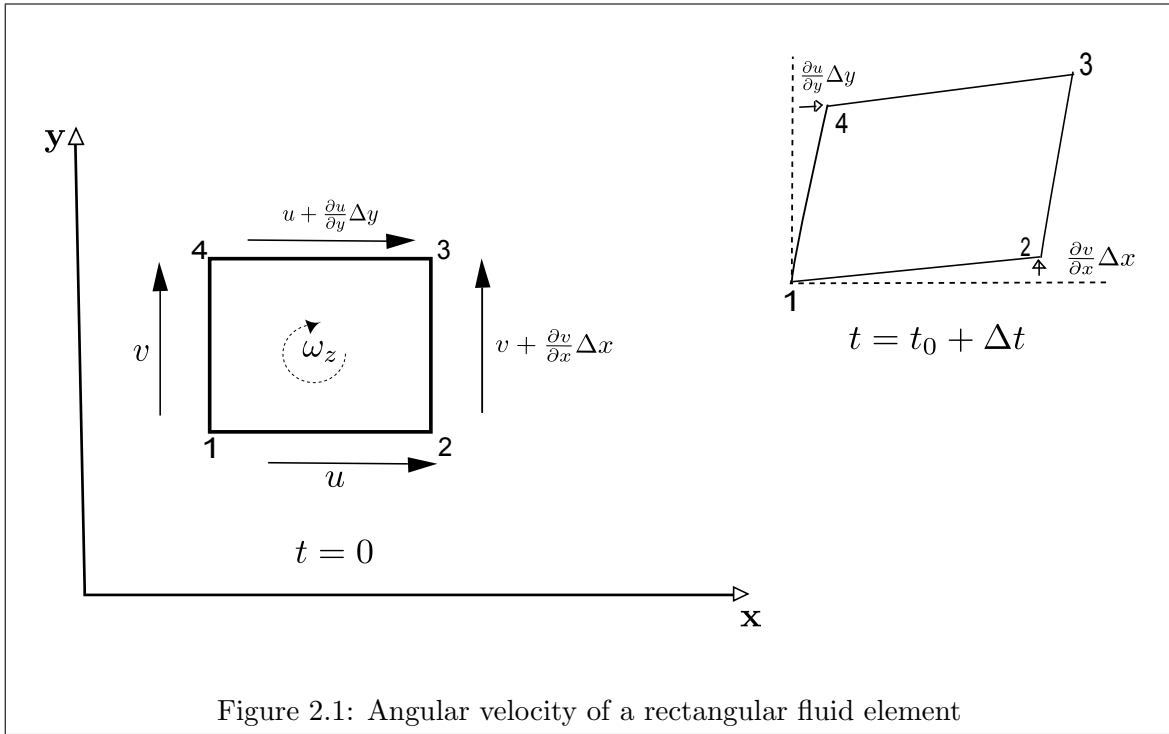


Figure 2.1: Angular velocity of a rectangular fluid element

$$\underline{w}_z = \frac{w_{1-2} + w_{1-4}}{2} \quad (2.4)$$

$$\underline{w}_z = \frac{1}{2} \left(\frac{\partial v}{\partial x} - \frac{\partial u}{\partial y} \right) \quad (2.5)$$

Note that the angular velocity is perpendicular to the xy -plane where the fluid element lies.

The w_x and w_y components of the angular velocity can be derived in a similar fashion as performed above. The angular velocity then becomes

$$\underline{w} = \frac{1}{2} (\underline{\nabla} \times \underline{q}) \quad (2.6)$$

$$\underline{w} = \frac{1}{2} \begin{vmatrix} \underline{i} & \underline{j} & \underline{k} \\ \frac{\partial}{\partial x} & \frac{\partial}{\partial y} & \frac{\partial}{\partial z} \\ u & v & w \end{vmatrix} = \frac{1}{2} \begin{pmatrix} \frac{\partial w}{\partial y} - \frac{\partial v}{\partial z} \\ \frac{\partial u}{\partial z} - \frac{\partial w}{\partial x} \\ \frac{\partial v}{\partial x} - \frac{\partial u}{\partial y} \end{pmatrix} \quad (2.7)$$

In the above equation $\underline{\nabla}$ represents the nabla operator or gradient vector, and \underline{q} is the velocity vector. In our notation underlined characters represent vector quantities.

2.1.1 Vorticity

We will define the vorticity ζ as two times the angular velocity. The vorticity as a vector will also have three components.

$$\underline{\zeta} = 2\underline{\omega} = \underline{\nabla} \times \underline{V} \quad (2.8)$$

$$\underline{\zeta}_x = \left(\frac{\partial w}{\partial y} - \frac{\partial v}{\partial z} \right) (\hat{i}) \quad (2.9)$$

$$\underline{\zeta}_y = \left(\frac{\partial u}{\partial z} - \frac{\partial w}{\partial x} \right) (\hat{j}) \quad (2.10)$$

$$\underline{\zeta}_z = \left(\frac{\partial v}{\partial x} - \frac{\partial u}{\partial y} \right) (\hat{k}) \quad (2.11)$$

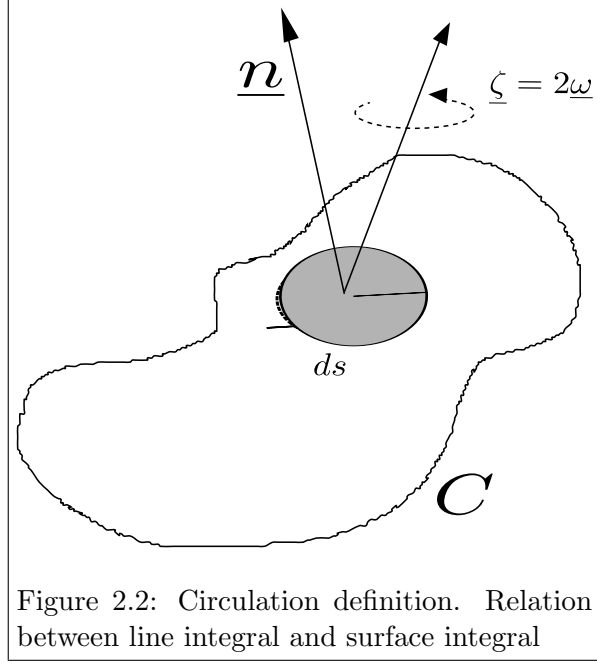
2.1.2 Circulation

In order to define the circulation, consider the open surface S from figure 2.2. The surface S has the closed curve C as its boundary. Stokes' theorem states that the vorticity on the surface S can be related to the line integral around C in order to obtain the circulation as follows:

$$\Gamma = \iint_S \underline{\zeta} \cdot \underline{n} ds = \iint_S (\underline{\nabla} \times \underline{q}) \cdot \underline{n} ds = \oint_C \underline{q} \cdot \underline{dl} \quad (2.12)$$

In the above equation \underline{n} is the normal vector to the surface S . The line integral on the right hand side of Stokes' theorem expression in equation 2.12 is called the circulation Γ .

The relation stated in Stokes' theorem can be illustrated using the fluid element from figure 2.1. Since we have an infinitesimal fluid element we will compute the delta circulation $\Delta\Gamma$, corresponding to the element by evaluating the line integral of the tangential velocity components along the edges around the fluid element. We will use a sign convention following the positive direction of the angular velocity $\underline{\omega}$:



$$\begin{aligned}
\Delta\Gamma &= \oint_C \underline{q} \cdot \underline{dl} \\
&= u(\Delta x) + \left(v + \frac{\partial v}{\partial x} \Delta x \right) (\Delta y) - \left(u + \frac{\partial u}{\partial y} \Delta y \right) (\Delta x) - v(\Delta y) \\
&= \frac{\partial v}{\partial x} \Delta x \Delta y - \frac{\partial u}{\partial y} \Delta x \Delta y \\
\Delta\Gamma &= \oint_C \underline{q} \cdot \underline{dl} = \left(\frac{\partial v}{\partial x} - \frac{\partial u}{\partial y} \right) \Delta x \Delta y \\
&= \iint_S \underline{\zeta}_z ds
\end{aligned} \tag{2.13}$$

Note that in equation 2.13 the product $[\Delta x \Delta y]$ represents the delta area ΔA or ds of the infinitesimal fluid element, and $[(\partial v / \partial x) - (\partial u / \partial y)]$ is the vorticity.

Comparing the result of equation 2.13 with the result of the integral of the vorticity over the surface of the infinitesimal fluid element we get:

$$\iint_S \underline{\zeta} \cdot \underline{nds} = \iint_S (\nabla \times \underline{q}) \cdot \underline{nds} = \left(\frac{\partial v}{\partial x} - \frac{\partial u}{\partial y} \right) \Delta x \Delta y = \oint_C \underline{q} \cdot \underline{dl} = \Delta\Gamma \tag{2.14}$$

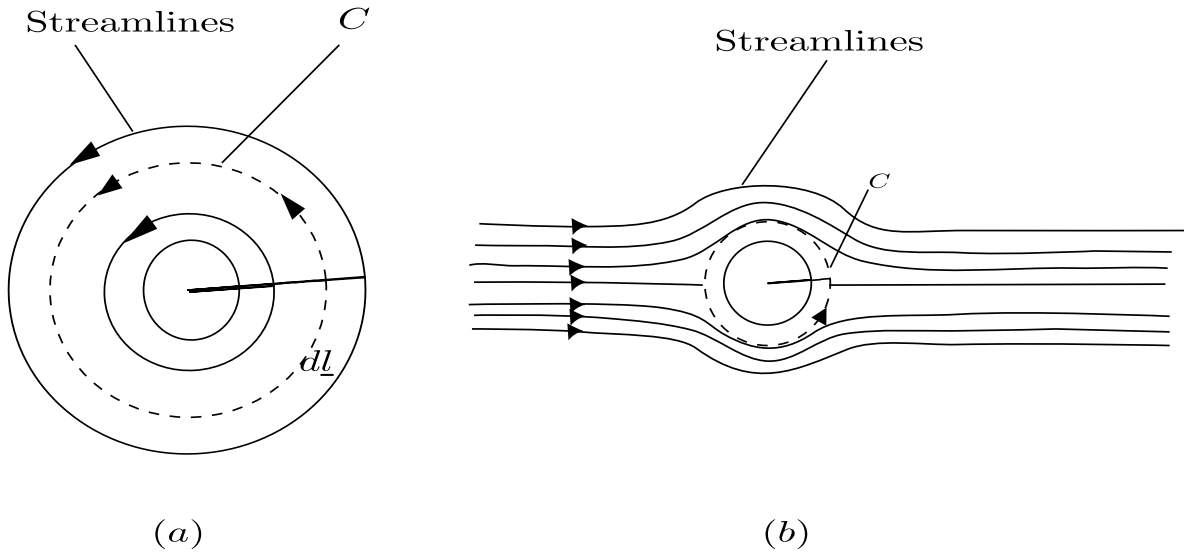


Figure 2.3: Flow field with circulation (a) and without circulation (b)

As a general remark note that $\underline{n} \cdot d\mathbf{s} = d\mathbf{s}$. Additionally, note that in the above equation we wrote $\Delta\Gamma$ to refer to the circulation Γ of an infinitesimal element with area $d\mathbf{s}$. For the general 3D case we can write the circulation as

$$\Gamma = \iint_S \underline{\zeta} \cdot \underline{n} ds = \iint_S (\underline{\nabla} \times \underline{q}) \cdot \underline{n} ds = \oint_C \underline{q} \cdot d\mathbf{l} \quad (2.15)$$

So far we have learned that the circulation is related to the rotation in the fluid (e.g. to the angular velocity of a solid body type rotation). In figure 2.3(a) we observe that along the circular integration path C (dashed line), since the velocity \underline{q} and $d\mathbf{l}$ are positive for all $d\mathbf{l}$, in this case we will have a positive circulation. In figure 2.3(b) the flow field is the symmetric flow of a uniform stream past a circular cylinder. It is clear from the symmetry that when integrating the velocity \underline{q} around the circular path $d\mathbf{l}$ (dashed line) we will get a zero circulation.

For irrotational flow the curl of the velocity vector \underline{q} (or cross product between the nabla operator and the velocity) is equal to zero [$\underline{\nabla} \times \underline{q} = 0$] which means that:

$$\begin{aligned} \frac{\partial w}{\partial y} &= \frac{\partial v}{\partial z} \\ \frac{\partial u}{\partial z} &= \frac{\partial w}{\partial x} \\ \frac{\partial v}{\partial x} &= \frac{\partial u}{\partial y} \end{aligned} \quad (2.16)$$

Also, note that for irrotational flow the integral of the dot product between the velocity \underline{q} and \underline{dl} is zero [$\oint_C \underline{q} \cdot \underline{dl} = 0$], around the curve contour C .

2.1.3 Rate of Change of vorticity

We want to obtain an equation for the rate of change of the vorticity for a fluid element. We start with the incompressible Navier-Stokes equation

$$\frac{\partial \underline{q}}{\partial t} + \underline{q}^T \cdot \nabla \underline{q} = \underline{f} - \nabla \frac{P}{\rho} + \nu \nabla^2 \underline{q} \quad (2.17)$$

We can also write equation 2.17 as follows:

$$\frac{\partial \underline{q}}{\partial t} + \underline{q}^T \cdot \nabla \underline{q} = \underline{f} - \nabla \frac{P}{\rho} + \nu \Delta \underline{q} \quad (2.18)$$

In the above equation Δ is the laplace operator $\nabla^2 = \Delta$.

To obtain the rate of change of vorticity we will use the following vector identity:

$$(\underline{q}^T \cdot \nabla) \underline{q} = \nabla \left(\frac{1}{2} \underline{q}^2 \right) - \underline{q} \times (\nabla \times \underline{q}) \quad (2.19)$$

We can substitute the curl of the velocity with the vorticity $|\nabla \times \underline{q}| = \underline{\zeta}$ in the above vector identity

$$(\underline{q}^T \cdot \nabla) \underline{q} = \nabla \left(\frac{1}{2} \underline{q}^2 \right) - \underline{q} \times \underline{\zeta} \quad (2.20)$$

Substituting the right hand side of equation 2.20 in to eq. 2.18 yields:

$$\frac{\partial \underline{q}}{\partial t} + \nabla \left(\frac{1}{2} \underline{q}^2 \right) - \underline{q} \times \underline{\zeta} = \underline{f} - \nabla \frac{P}{\rho} + \nu \Delta \underline{q} \quad (2.21)$$

Now we will perform a cross product between the nabla operator ∇ and each of the terms on the above equation 2.21:

$$\nabla \times \left[\frac{\partial \underline{q}}{\partial t} + \nabla \left(\frac{1}{2} \underline{q}^2 \right) - \underline{q} \times \underline{\zeta} \right] = \nabla \times \left[\underline{f} - \nabla \frac{P}{\rho} + \nu \Delta \underline{q} \right] \quad (2.22)$$

Applying the cross product between the gradient $[\nabla]$, or nabla operator, and each term of the equation yields:

$$\nabla \times \frac{\partial \underline{q}}{\partial t} + \nabla \times \left[\nabla \left(\frac{1}{2} \underline{q}^2 \right) \right] - \nabla \times (\underline{q} \times \underline{\zeta}) = \nabla \times \underline{f} - \nabla \times \left(\frac{\nabla P}{\rho} \right) + \nabla \times (\nu \Delta \underline{q}) \quad (2.23)$$

Before performing the cross product in each term of equation 2.23, recall that the cross product or curl of a vector by itself yields zero:

$$|\underline{A} \times \underline{B}| = |A| |B| \sin\theta \quad (2.24)$$

$$|\underline{A} \times \underline{A}| = |A| |A| \sin(0) \quad (2.25)$$

$$|\underline{A} \times \underline{A}| = 0 \quad (2.26)$$

In equation 2.24 $[\theta]$ is the angle between the vectors $[\underline{A}]$ and $[\underline{B}]$

Now analysing each of the cross products on the different terms of eq 2.23 we get

$$\left[\nabla \times \frac{\partial \underline{q}}{\partial t} \right] = \frac{\partial}{\partial t} (\nabla \times \underline{q}) = \frac{\partial \underline{\zeta}}{\partial t} \quad (2.27)$$

$$\nabla \times \left[\nabla \left(\frac{1}{2} \underline{q}^2 \right) \right] = (\nabla \times \nabla) \frac{1}{2} \underline{q}^2 = 0 \quad (2.28)$$

$$\nabla \times (\underline{q} \times \underline{\zeta}) = \nabla \times (\underline{q} \times \underline{\zeta}) \quad (2.29)$$

$$\nabla \times \underline{f} = \nabla \times \underline{f} \quad (2.30)$$

$$\nabla \times \left(\frac{\nabla P}{\rho} \right) = (\nabla \times \nabla) \frac{P}{\rho} = 0 \quad (2.31)$$

$$\nabla \times (\nu \Delta \underline{q}) = \nu \Delta (\nabla \times \underline{q}) = \nu \Delta \underline{\zeta} \quad (2.32)$$

Then equation 2.23 will yield

$$\frac{\partial \underline{\zeta}}{\partial t} - \nabla \times (\underline{q} \times \underline{\zeta}) = \nabla \times \underline{f} + \underline{\zeta} \nu \Delta \quad (2.33)$$

To further simplify the result obtained in the equation above we use the following vector identity:

$$\nabla \times (\underline{q} \times \underline{\zeta}) = \underline{q}(\nabla^T \cdot \underline{\zeta}) - (\underline{q}^T \cdot \nabla)\underline{\zeta} + (\underline{\zeta}^T \cdot \nabla)\underline{q} - \underline{\zeta}(\nabla^T \cdot \underline{q}) \quad (2.34)$$

Now, if we recall the continuity equation for incompressible flow $[\nabla \cdot \underline{q} = 0]$, and also consider that the vorticity is divergence free: $[\nabla \times \underline{q} = \underline{\zeta}]$ and $[\nabla \cdot (\nabla \times \underline{q}) = 0]$ (The dot product

of two perpendicular vectors is zero, and the gradient and the vorticity are perpendicular). We get from the vector identity in eq 2.34:

$$\underline{q} (\underline{\nabla}^T \cdot \underline{\zeta}) = \underline{q} [\underline{\nabla}^T \cdot (\underline{\nabla} \times \underline{q})] = 0 \quad (2.35)$$

$$(\underline{q}^T \cdot \underline{\nabla}) \underline{\zeta} = 0, \quad (\text{but we will keep this term for convenience}) \quad (2.36)$$

$$(\underline{\zeta}^T \cdot \underline{\nabla}) \underline{q} = \left((\underline{\nabla} \times \underline{q})^T \cdot \underline{\nabla} \right) \underline{q} = 0 \quad (2.37)$$

$$\underline{\zeta} (\underline{\nabla} \cdot \underline{q}) = 0 \quad (2.38)$$

Additionally, we will assume that the body force acting is conservative and thus its curl is zero $[\underline{\nabla} \times \underline{f} = 0]$

Then, as a result we get for equation 2.33:

$$\frac{\partial \underline{\zeta}}{\partial t} + (\underline{q}^T \cdot \underline{\nabla}) \underline{\zeta} = \nu \Delta \underline{\zeta} \quad (2.39)$$

Now, recalling the expression for the total differential:

$$\frac{D \underline{\zeta}}{Dt} = \frac{\partial \underline{\zeta}}{\partial t} + (\underline{q}^T \cdot \underline{\nabla}) \underline{\zeta} = \nu \Delta \underline{\zeta} \quad (2.40)$$

If we assume an inviscid flow with no viscosity $[\nu = 0]$, then from eq 2.40 we get:

$$\frac{D \underline{\zeta}}{Dt} = 0 \quad (2.41)$$

Equation 2.41 states that the rate of change of vorticity for each fluid element remains constant.

2.1.4 Kelvin's Theorem: Rate of change of Circulation

The circulation Γ around a closed fluid curve C which remains static in the fluid domain, in an incompressible, inviscid flow, with conservative forces acting, takes the form

$$\oint_C \underline{q} \cdot \underline{dl} = \Gamma \quad (2.42)$$

Then, the rate of change of the circulation would take the form:

$$\frac{D \Gamma}{Dt} = \frac{D}{Dt} \oint_C \underline{q} \cdot \underline{dl} = \oint_C \frac{D \underline{q}}{Dt} \cdot \underline{dl} + \oint_C \underline{q} \cdot \frac{D \underline{dl}}{Dt} \quad (2.43)$$

Additionally, we have that for the acceleration \underline{a} and the velocity \underline{q}

$$\frac{D\underline{q}}{Dt} = \underline{a} \quad \text{and} \quad \frac{D}{Dt}\underline{dl} = \underline{dq} \quad (2.44)$$

As a result, we can write

$$\frac{D\underline{\Gamma}}{Dt} = \oint_C \underline{a} \cdot \underline{dl} + \oint_C \underline{q} \cdot \underline{dq} \quad (2.45)$$

Note that for a closed integral of an exact differential [$\oint_C \underline{q} \cdot \underline{dq} = \oint_C \underline{dq}^2/2 = 0$], thus from eq 2.41 we get

$$\frac{D\underline{\Gamma}}{Dt} = \oint_C \underline{a} \cdot \underline{dl} \quad (2.46)$$

We can obtain the acceleration \underline{a} from Euler's equation as follows

$$\frac{D\underline{q}}{Dt} = \frac{\partial \underline{q}}{\partial t} + (\underline{q}^T \cdot \nabla) \underline{q} = \underline{a} = \underline{f} - \nabla \left(\frac{p}{\rho} \right) \quad (2.47)$$

Then,

$$\underline{a} = -\nabla \left(\frac{p}{\rho} \right) + \underline{f} \quad (2.48)$$

Now, if we substitute equation 2.48 into equation 2.46 yields

$$\frac{D\underline{\Gamma}}{Dt} = \oint_C \left(\underline{f} - \nabla \left(\frac{p}{\rho} \right) \right) \cdot \underline{dl} \quad (2.49)$$

which results in

$$\frac{D\underline{\Gamma}}{Dt} = \oint_C \underline{f} \cdot \underline{dl} - \oint_C d \left(\frac{p}{\rho} \right) \underline{dl} \quad (2.50)$$

The first integral of the above equation will vanish because the work done by a conservative force around a closed path is zero [$\oint_C \underline{f} \cdot \underline{dl} = 0$]. The second integral will also vanish for being the closed integral of an exact differential. As a result, the time rate of change of vorticity around a closed curve static in the flow domain is zero for an inviscid, incompressible fluid. This statement is known as Kelvin's Theorem.

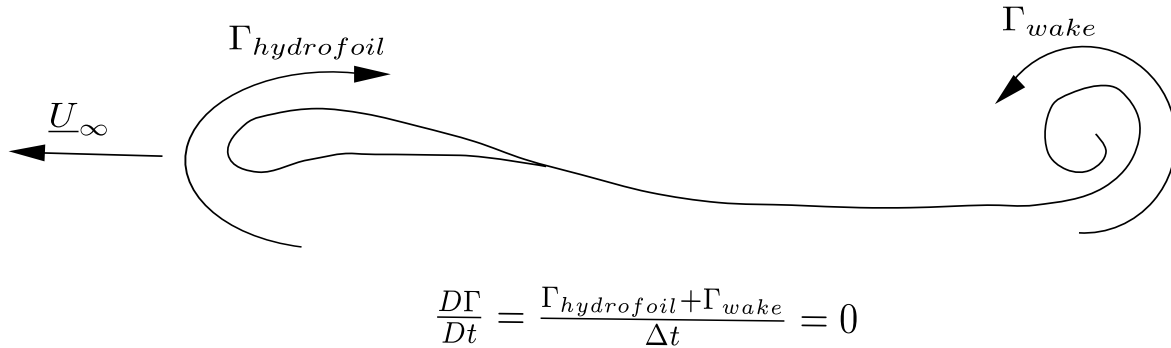


Figure 2.4: Circulation produced by a foil after it starts moving

Kelvin's theorem has interesting implications. For instance, a hydrofoil which is at rest at a time t_0 , will develop some circulation around it after it starts advancing forward steadily at a time t_1 . In order to comply with Kelvin's theorem a vortex wake circulation Γ_{Wake} must exist, so that the total circulation around the foil and the wake is zero; as it was before the foil movement started. See figure 2.4

$$\frac{D\Gamma}{Dt} = \frac{1}{\Delta t} (\Gamma_{Foil} + \Gamma_{Wake}) = 0 \quad (2.51)$$

2.1.5 Vortex Quantities

In our fluids mechanics background we have seen some quantities related to the velocity vector \underline{q} , like streamlines, stream tubes, and stream forces. Now, we will define similar quantities related to the vorticity vector.

Vortex Lines

We will define the vortex lines as the field lines that are parallel to the vorticity vector. We can describe a vortex line mathematically as follows:

$$\underline{\zeta} \times \underline{dl} = 0 \quad (2.52)$$

where \underline{dl} is a segment along the vortex line. See figure 2.5. Performing the cross product in equation 2.52, we get the differential equation for vortex line in Cartesian coordinates:

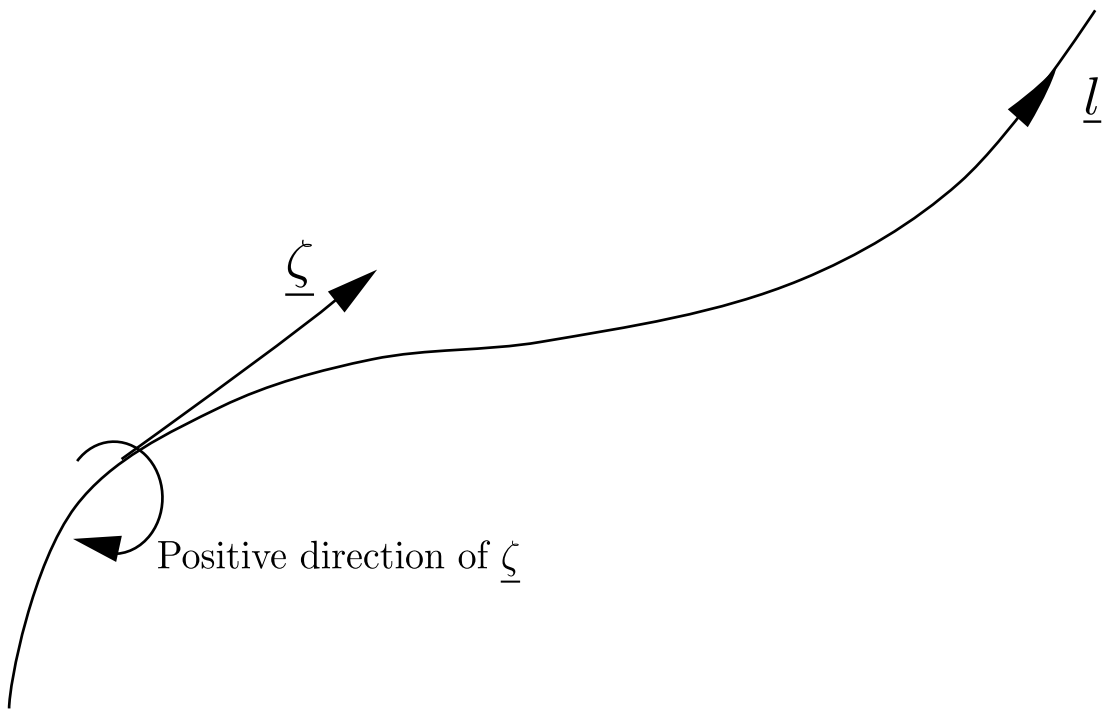


Figure 2.5: vortex line

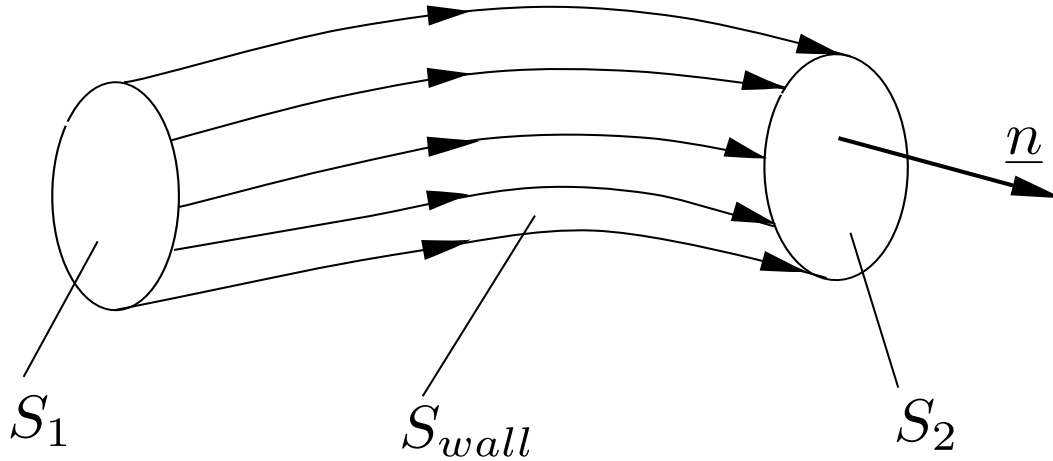


Figure 2.6: Vortex tube

$$\frac{dx}{\zeta_{\hat{i}}} = \frac{dy}{\zeta_{\hat{j}}} = \frac{dz}{\zeta_{\hat{k}}} \quad (2.53)$$

Vortex Surface

When several vortex lines pass through an open curve in space, they form a vortex surface.

Vortex Tube

When several vortex lines pass through a closed curve in space they form a vortex tube. See figure 2.6

Vortex Filament

A vortex filament is defined as vortex tube with infinitesimal cross sectional area.

Recall that the divergence of vorticity is zero $[\nabla \cdot \underline{\zeta} = 0]$ because the divergence of the curl of any vector is zero $[\nabla \cdot \underline{\zeta} = \nabla \cdot (\nabla \times \underline{\zeta}) = 0]$.

If we apply the divergence theorem to a region in space R surrounded by a surface \underline{S} , we get:

$$\iint_S \underline{\zeta} \cdot \underline{n} ds = \iiint_R \underline{\nabla} \cdot \underline{\zeta} dv = 0 \quad (2.54)$$

Applying equation 2.54 at an instant of time to a vortex tube formed by the surfaces S_w which is the tube side wall, and the tube caps S_1 and S_2 . See Figure 2.6. The equation takes the form:

$$-\iint_{S_1} \underline{\zeta} \cdot \underline{n} ds + \iint_{S_2} \underline{\zeta} \cdot \underline{n} ds + \iint_{S_w} \underline{\zeta} \cdot \underline{n} ds = \iiint_R \underline{\nabla} \cdot \underline{\zeta} dv = 0 \quad (2.55)$$

The surface integral over $[S_w]$ vanishes because the vorticity vector and the surface normal vector are perpendicular $[\underline{\zeta} \perp \underline{n}]$, thus, their dot product is zero $[\underline{\zeta} \cdot \underline{n} = 0]$. Then, for the above equation we are left with:

$$\iint_{S_1} \underline{\zeta} \cdot \underline{n} ds = \iint_{S_2} \underline{\zeta} \cdot \underline{n} ds = \text{const.} \quad (2.56)$$

Additionally, recall that

$$\iint_S \underline{\zeta} \cdot \underline{n} ds = \Gamma_C \quad (2.57)$$

We can then conclude that at any instance of time the circulation will be constant $\Gamma = \text{const}$ for any cross sectional surface along the vortex tube. If we take C as any closed curve surrounding the vortex tube and lies on the tube wall, then the circulation around the curve C will be constant for any location of C along the vortex tube.

$$\iint_S \underline{\zeta} \cdot \underline{n} ds = \Gamma_C = \text{const} \quad (2.58)$$

Note that for each vortex filament $\Gamma_C = \underline{\zeta} \cdot \underline{ds} = \text{const.}$ and the vorticity of each vortex filament is inversely proportional to its cross sectional area. This means that for a constant circulation Γ_C a zero vortex filament area $\underline{ds} = 0$ would imply an infinite vorticity $\underline{\zeta} = \infty$. Based on this fact we can state that a vortex filament cannot start nor end in the fluid.

The above findings along with those we have seen like the time rate of change of circulation (see Section 2.43) were captured in what are called Helmholtz vortex theorems:

1. The strength of a vortex filament is constant across its length.
2. A vortex filament cannot end nor start in the fluid. It must form a closed path or extend to infinity.

3. The fluid that forms a vortex tube continues to form a vortex tube and the strength of the vortex tube remains constant as the tube moves around. Then, vortex elements will remain vortex elements with time, i.e. vortex lines, vortex tubes, vortex surfaces.

2.1.6 Two Dimensional Vortex

The flow field called two-dimensional vortex can be explained and depicted by considering a rigid two-dimensional cylinder with radius $[R]$ which rotates with constant angular velocity $\underline{\omega}_y$ in a viscous fluid. The cylinder rotational motion will produce a flow with cylindrical streamlines. See figure 2.7. For this flow pattern the radial velocity component will be zero. As a result, we have that the continuity equation in the $r, \theta - plane$ takes the form:

$$\frac{\partial \underline{q}_\theta}{\partial \theta} = 0 \quad (2.59)$$

Integrating equation 2.59 we get

$$\underline{q}_\theta = q_\theta(r) \quad (2.60)$$

The above equation means that the tangential velocity component $[q_\theta]$ is a function only of the radius $[r]$. We can easily visualize this if we recall that $[\underline{q}_\theta = \underline{\omega}_y \times \underline{r}]$. Then, given that the angular velocity is constant $[\underline{\omega}_y = const]$, then $[q_\theta]$ is only a function of the radius $[r]$.

Recall the Navier - Stokes equation for an incompressible fluid in the $r - direction$, in cylindrical coordinates

$$\rho \left(\frac{Dq_r}{Dt} - \frac{q_\theta^2}{r} \right) = \rho f_r - \frac{\partial p}{\partial r} + \mu \left(\nabla^2 q_r - \frac{q_r}{r^2} - \frac{2}{r^2} \frac{\partial q_\theta}{\partial \theta} \right) \quad (2.61)$$

The Navier - Stokes equation for an incompressible fluid in the $\theta - direction$

$$\rho \left(\frac{Dq_\theta}{Dt} - \frac{q_\theta q_r}{r} \right) = \rho f_\theta - \frac{1}{r} \frac{\partial p}{\partial \theta} + \mu \left(\nabla^2 q_\theta - \frac{q_\theta}{r^2} + \frac{2}{r^2} \frac{\partial q_r}{\partial \theta} \right) \quad (2.62)$$

The Navier - Stokes equation for an incompressible fluid in the $z - direction$

$$\rho \frac{Dq_z}{Dt} = \rho f_z - \frac{\partial p}{\partial z} + \mu \nabla^2 q_z \quad (2.63)$$

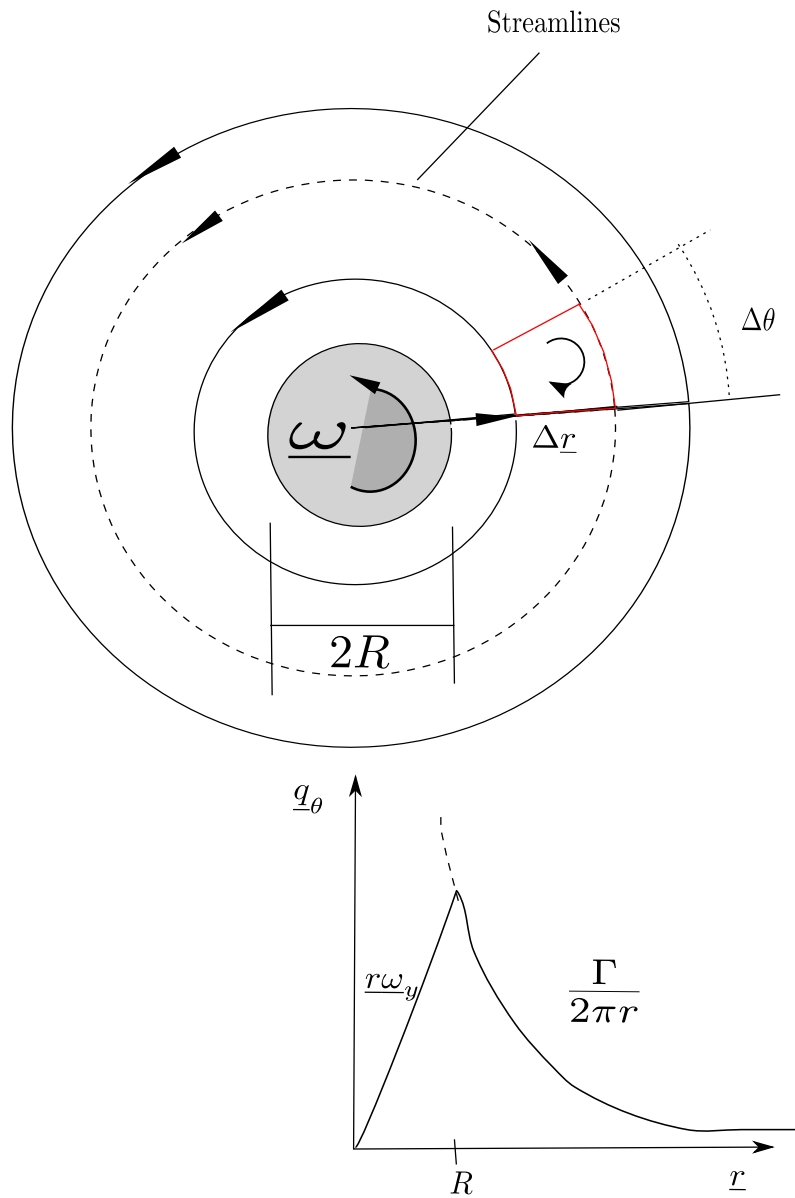


Figure 2.7: Two dimensional vortex produced by a rotating cylindrical core

So far we have that the tangential velocity \underline{q}_θ is only a function of the radius \underline{r} . Additionally, because of the radial symmetry of the flow, the pressure p must be either a constant or a function of the radius $p = p(r)$. As a consequence, the derivative of the pressure will not appear in the momentum equation in the $\underline{\theta}$ – *direction*. Also, neglecting the body forces f_θ , we get for each term of equation 2.62:

$$\frac{\underline{q}_\theta^T \cdot \underline{q}_r}{\underline{r}} = 0 \quad \text{Because} \quad \underline{q}_r = 0 \quad (2.64a)$$

$$\frac{D\underline{q}_\theta}{Dt} = 0 \quad \text{Because} \quad \underline{q}_\theta = \text{const} \quad \text{for a given radius} \quad (2.64b)$$

$$\rho f_\theta = 0 \quad \text{Because the body forces are neglected} \quad (2.64c)$$

$$\frac{1}{r} \frac{\partial p}{\partial \theta} = 0 \quad \text{Because} \quad p = p(r) \quad \text{or} \quad p = \text{const} \quad (2.64d)$$

Note that in equation 2.64b we can say that \underline{q}_θ is only function of the radius and not a function of time because the rotational velocity of the cylinder is constant $\omega = \text{const}$.

Then, in the θ – *direction* we are left with

$$\mu \left(\nabla^2 \underline{q}_\theta - \frac{\underline{q}_\theta}{r^2} \right) = 0 \quad (2.65)$$

In the case of the Navier-Stokes' equation in the r – *direction*, and after reducing terms we get

$$-\rho \frac{\underline{q}_\theta}{\underline{r}} = -\frac{\partial p}{\partial r} \quad (2.66)$$

In equation 2.65 we have to apply the Laplace operator Δ to the tangential velocity $[\underline{q}_\theta]$ as follows $[\nabla^2 \underline{q}_\theta = (\nabla^T \cdot \nabla) \underline{q}_\theta = \Delta \underline{q}_\theta]$. First recall the expression for the Laplace operator in cylindrical coordinates

$$\nabla^2 = \Delta = \frac{\partial^2}{\partial r^2} + \frac{1}{\underline{r}} \frac{\partial}{\partial r} + \frac{1}{r^2} \frac{\partial^2}{\partial \theta^2} + \frac{\partial^2}{\partial z^2} \quad (2.67)$$

Then, expanding the equation 2.65 we get:

$$\mu \left(\frac{\partial^2 \underline{q}_\theta}{\partial r^2} + \frac{1}{\underline{r}} \frac{\partial \underline{q}_\theta}{\partial r} + \frac{1}{r^2} \frac{\partial^2 \underline{q}_\theta}{\partial \theta^2} + \frac{\partial^2 \underline{q}_\theta}{\partial z^2} - \frac{\underline{q}_\theta}{r^2} \right) = 0 \quad (2.68)$$

Finally, considering that the tangential velocity q_θ is constant along the cylinder axis, since this is a 2-D vortex problem, and also considering the facts pointed out in eq 2.64, we get:

$$\mu \left(\frac{\partial^2 q_\theta}{\partial r^2} + \frac{1}{r} \frac{\partial q_\theta}{\partial r} - \frac{q_\theta}{r^2} \right) = 0 \quad (2.69)$$

In the above equation since q_θ is only function of r we can write the partial derivative as total derivatives

$$\mu \left(\frac{d^2 q_\theta}{dr^2} + \frac{1}{r} \frac{dq_\theta}{dr} - \frac{q_\theta}{r^2} \right) = 0 \quad (2.70)$$

Additionally, note that

$$\frac{d}{dr} \left(\frac{q_\theta}{r} \right) = \frac{r \left(\frac{dq_\theta}{dr} \right) - q_\theta \left(\frac{dr}{dr} \right)}{r^2} = \frac{1}{r} \frac{dq_\theta}{dr} - \frac{q_\theta}{r^2} \quad (2.71)$$

Then, we can write equation 2.70 as follows

$$\frac{d^2 q_\theta}{dr^2} + \frac{d}{dr} \left(\frac{q_\theta}{r} \right) = 0 \quad (2.72)$$

Now, if we integrate the equation 2.72 with respect to r we will get

$$\frac{dq_\theta}{dr} + \frac{q_\theta}{r} = C_1 \quad (2.73)$$

where C_1 is the constant of integration. We can re-arrange equation 2.73 as follows

$$\frac{1}{r} \frac{d}{dr} \left(r q_\theta \right) = C_1 \quad (2.74)$$

An additional integration will yield, but reorganizing again first:

$$\int \frac{d}{dr} \left(r q_\theta \right) dr = \int r C_1 dr \quad (2.75)$$

$$\left(r q_\theta \right) = \frac{C_1 r^2}{2} + C_2 \quad (2.76)$$

$$\underline{q}_\theta = \frac{C_1 r}{2} + \frac{C_2}{r} \quad (2.77)$$

To find out the value of the constants on equation 2.77 we will use the boundary conditions of the problem. The flow produced by the rotating cylinder will have as a boundary condition that at $[r = R]$ the tangential velocity will be $[\underline{q}_\theta = -R \omega_y]$. The other boundary condition will be that the flow field created will vanish at infinity. $[\underline{q}_\theta = 0 \text{ for } r = \infty]$.

Substituting the second boundary condition in equation 2.77 will yield

$$\underline{q}_\theta = 0 = \frac{C_1 \infty}{2} + \frac{C_2}{\infty} \quad (2.78)$$

Thus, we note that $[C_1 = 0]$. Then, substituting the first boundary condition $[\underline{q}_\theta = -R \omega_y]$ for $[r = R]$ we get

$$\underline{q}_\theta = -R \omega_y = \frac{C_2}{R} \text{ for } r = R \quad (2.79a)$$

$$-R^2 \omega_y = C_2 \quad (2.79b)$$

Finally, substituting the values of $[C_1]$ and $[C_2]$ in equation 2.77 we get for the tangential velocity

$$\underline{q}_\theta = -\frac{R^2 \omega_y}{r} \quad (2.80)$$

After finding the tangential velocity for the 2-D vortex flow produced by a rotating cylinder of radius R , we will now find the circulation around a circle of radius $[r]$ concentric with the cylinder and with larger radius. We will use equation 2.12

$$\Gamma = \oint \underline{q} dl = \int_{2\pi}^0 \underline{q}_\theta (r d\theta) \quad (2.81)$$

Substituting the tangential velocity $[\underline{q}_\theta]$ in the above equation we get

$$\Gamma = \oint \underline{q} dl = \int_{2\pi}^0 \frac{\omega_y R^2}{r} (r d\theta) = -2\pi R^2 \omega_y \quad (2.82)$$

Then, for the tangential velocity in terms of the circulation Γ we have

$$\underline{q}_\theta = \frac{\Gamma}{2\pi r} \quad (2.83)$$

In the vortex flow shown in figure 2.7 the tangential velocity \underline{q}_θ will become very large as r approaches zero $r \rightarrow 0$. It has been proved that the rotating cylinder produce a circulation Γ around it. It can be proved also that the flow is irrotational everywhere excluding the rotating cylinder at the boundary, where all the vorticity is generated. Take the red line path in figure 2.7 and look for the vorticity around the path. For this, recall that the radial velocity is zero for the vortex flow $\underline{q}_r = 0$:

$$\oint \underline{q} \cdot d\mathbf{l} = 0 \cdot \Delta r + \frac{\Gamma}{2\pi(r + \Delta r)} (r + \Delta r) \Delta\theta - 0 \cdot \Delta r - \frac{\Gamma}{2\pi r} r \Delta\theta = 0 \quad (2.84)$$

Additionally, we have to state that when the core size approaches zero $R \rightarrow 0$ the flow is called irrotational vortex, excluding at the core point where the tangential velocity approaches infinity. The vorticity will remain constant around the vortex.

2.1.7 The Biot - Savart Law

The Boit - Savart Law will help us determining the velocity field induced by a known vorticity distribution. For simplicity we will present here the resulting equation or formula. For a detailed derivation see Katz & Plotkin (2001). In the following equations \underline{r}_0 will be the vector representing the location of the point at which we want the velocity. \underline{r}_1 will represent the location where the vorticity is located. Both vectors are referenced to the origin of a global coordinate system.

$$\underline{q} = \frac{\Gamma}{4\pi} \int \frac{d\mathbf{l} \times (\underline{r}_0 - \underline{r}_1)}{|\underline{r}_0 - \underline{r}_1|^3} \quad (2.85)$$

or in differential form

$$\Delta \underline{q} = \frac{\Gamma}{4\pi} \frac{d\mathbf{l} \times (\underline{r}_0 - \underline{r}_1)}{|\underline{r}_0 - \underline{r}_1|^3} \quad (2.86)$$

Another expression for the Biot Savart Law is as follows

$$\underline{q} = \frac{\Gamma}{4\pi} \iiint \frac{\underline{\zeta} \times (\underline{r}_0 - \underline{r}_1)}{|\underline{r}_0 - \underline{r}_1|^3} dV \quad (2.87)$$

The above equation derives from the expression

$$\underline{q} = \frac{\Gamma}{4\pi} \iiint \nabla \times \frac{\underline{\zeta}}{|\underline{r}_0 - \underline{r}_1|^3} dV \quad (2.88)$$

2.1.8 The Velocity Induced by a straight vortex Segment

We have already seen that vortex lines cannot end nor start in the fluid. As a consequence, we will derive the influence or induced velocity by a segment of such vortex lines at a determined point \underline{P} in the fluid domain. For this, we will use the Biot Savart Law from the previous section.

Consider an arbitrary vortex segment with an arbitrary orientation. See figure 2.8. We can state a priori that the induced velocity will only have a tangential component as shown in the figure. From the Biot - Savart Law we have that

$$\Delta \underline{q} = \frac{\Gamma}{4\pi} \frac{d\underline{l} \times \underline{r}}{r^3} \quad (2.89)$$

We can write this in scalar form as follows

$$\Delta q_\theta = \frac{\Gamma}{4\pi} \frac{\sin\beta}{r^2} dl \quad (2.90)$$

If we look at the figure 2.8 we note that

$$d = r \sin\beta \quad \text{and} \quad \tan(\pi - \beta) = \frac{d}{l} \quad (2.91)$$

then,

$$l = \frac{-d}{\tan\beta} \quad \text{and} \quad dl = \frac{d}{\sin^2\beta} d\beta \quad (2.92)$$

If we substitute these in equation 2.90 yields

$$\Delta q_\theta = \frac{\Gamma}{4\pi} \frac{\sin^2\beta}{d^2} \sin\beta \frac{d}{\sin^2\beta} d\beta = \frac{\Gamma}{4\pi} \sin\beta d\beta \quad (2.93)$$

We can extend this equation and find the velocity induced by a segment [1 \rightarrow 2], with respective angles β_1 and β_2 , performing an integration. See figure 2.9

$$\Delta q_{\theta_{1-2}} = \frac{\Gamma}{4\pi d} \int_{\beta_1}^{\beta_2} \sin\beta d\beta = \frac{\Gamma}{4\pi d} (\cos\beta_1 - \cos\beta_2) \quad (2.94)$$

Note that for the 2D-case of an infinite vortex length we have that $\beta_1 = 0$ and $\beta_2 = \pi$. Therefore, the induced velocity will be

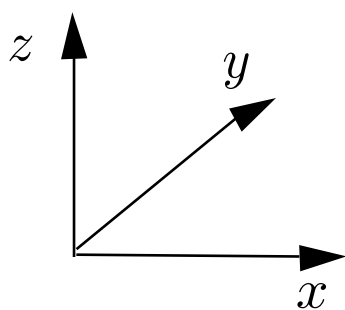
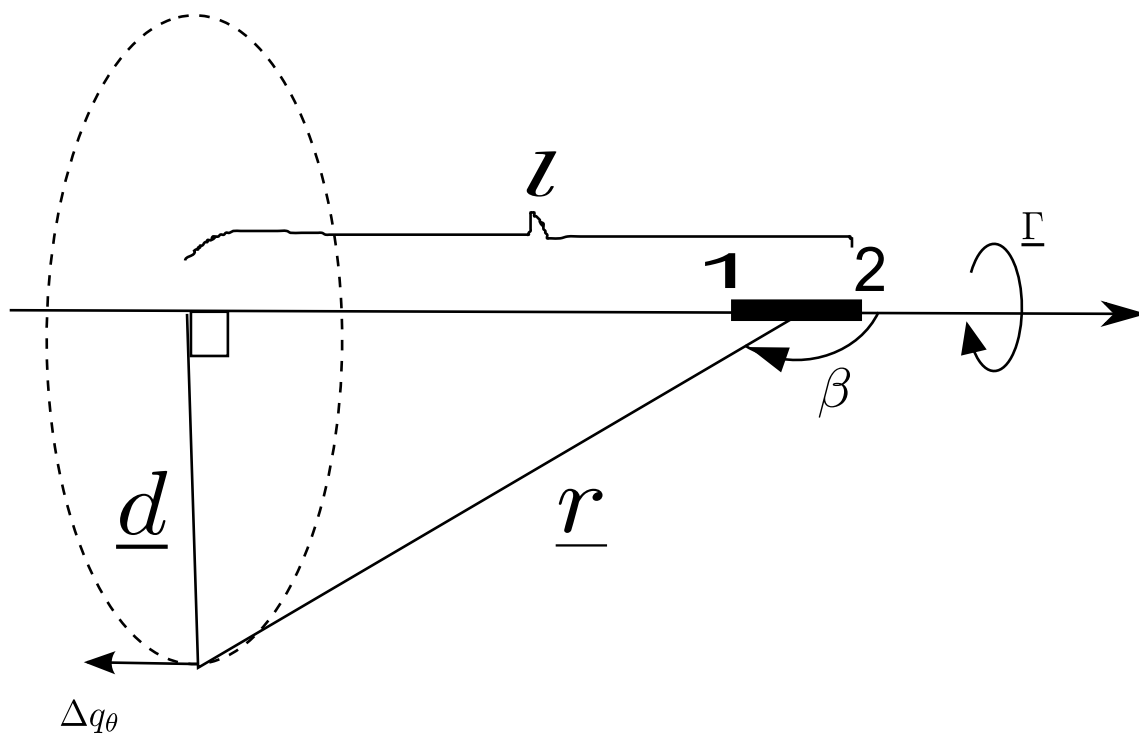


Figure 2.8: Velocity induced by a straight vortex segment

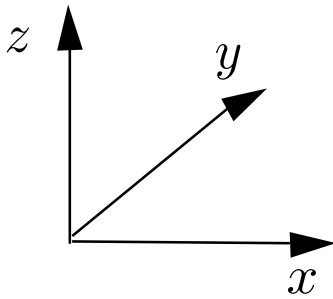
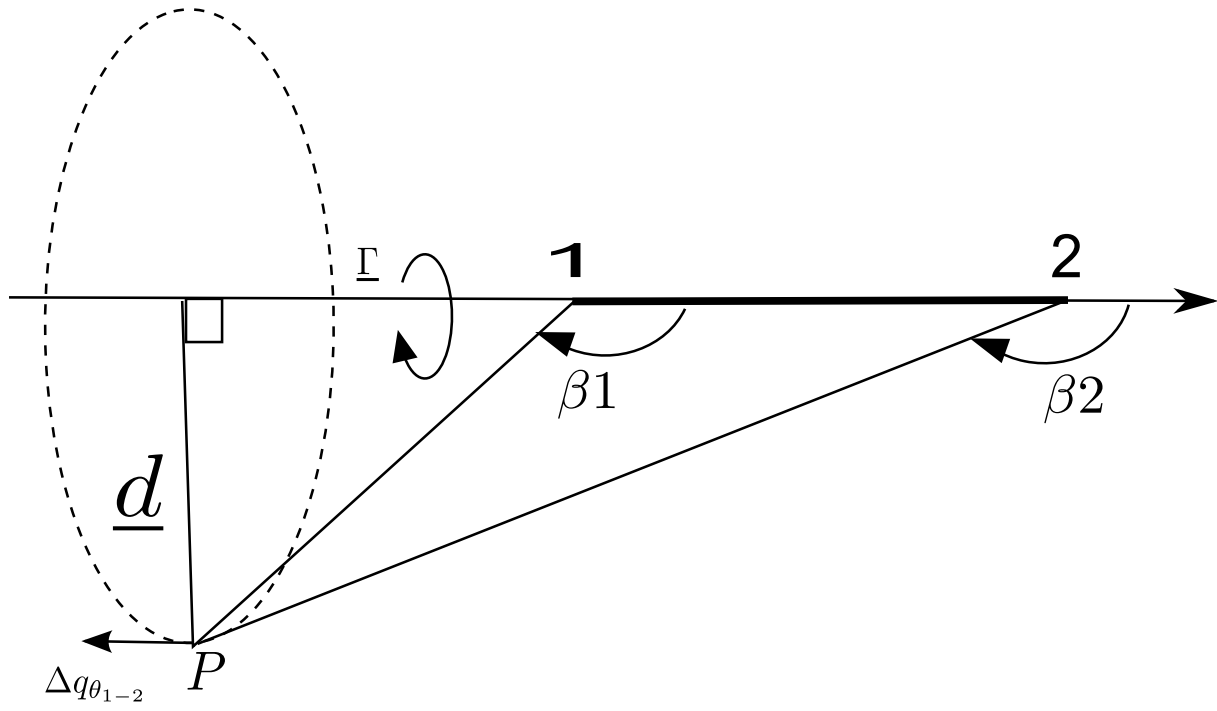


Figure 2.9: View angles for velocity induced by a straight vortex segment

$$q_\theta = \int_0^\pi \sin\beta \, d\beta = \frac{\Gamma}{2\pi d} \quad (2.95)$$

For a semi-infinite vortex segment with the line starting at point P_0 in figure 2.9 we have that $\beta_1 = \frac{\pi}{2}$ and $\beta_2 = \pi$, hence we get for the tangential velocity

$$q_\theta = \int_{\frac{\pi}{2}}^\pi \sin\beta \, d\beta = \frac{\Gamma}{4\pi d} \quad (2.96)$$

It will be useful for us, when conducting the implementation of a numerical solution for the lifting problem, to express equation 2.94 in vector form. In order to proceed note that

$$d = \frac{|r_1 \times r_2|}{r_0} \quad (2.97a)$$

$$\cos\beta_1 = \frac{|r_0 \cdot r_1|}{|r_0| |r_1|} \quad (2.97b)$$

$$\cos\beta_2 = \frac{|r_0 \cdot r_2|}{|r_0| |r_2|} \quad (2.97c)$$

We can observe that the velocity induced by the vortex segment will be perpendicular to the plane created by the point $[P]$ and the vertex edges [1] and [2]. The direction of the velocity will be given by

$$\frac{\underline{q}_\theta}{|\underline{q}_\theta|} = \frac{r_1 \times r_2}{|r_1 \times r_2|} \quad (2.98)$$

Using the above expressions and substituting them in equation 2.94 we get the vector equation for the velocity induced by a vortex segment

$$\underline{q}_{\theta_{1-2}} = \frac{\Gamma}{4\pi} \frac{r_1 \times r_2}{|r_1 \times r_2|^2} r_0 \cdot \left(\frac{r_1}{|r_1|} - \frac{r_2}{|r_2|} \right) \quad (2.99)$$

2.2 Equations and Solution for Incompressible Potential Flow

After the continuity equation (conservation of mass) and the Navier - Stokes Equations (momentum equations) are presented to us describing a fluid flow, there are some assumptions we can make in order to simplify these equations and use them to solve hydrodynamics problems and fluid flow problems in general. We will now briefly describe these assumptions and their physical interpretations.

Starting with the conservative, differential form, of the continuity equation we have

$$\frac{\partial \rho}{\partial t} + \nabla^T (\rho \underline{q}) = 0 \quad (2.100)$$

If we assume that the fluid is incompressible, with constant density $\rho = \text{const}$, we get the continuity equation for incompressible flow

$$\nabla^T (\underline{q}) = 0 \quad (2.101)$$

Now, if we take the Navier - Stokes vector equation for an incompressible fluid, which additionally has constant dynamic viscosity $\mu = \text{const}$, we get

$$\rho \left(\frac{\partial \underline{q}}{\partial t} + (\underline{q}^T \cdot \underline{\nabla}) \underline{q} \right) = \rho \underline{f} - \underline{\nabla} P + \mu (\underline{\nabla}^T \cdot \underline{\nabla} \underline{q}) + \frac{1}{3} \mu \underline{\nabla} (\underline{\nabla} \cdot \underline{q}) \quad (2.102)$$

For a detailed derivation of the continuity equation and the Navier - Stokes equation see Birk (2011).

From the continuity equation we have that $[\underline{\nabla}^T \cdot \underline{q} = 0]$. Also, recall that the kinematic viscosity ν is related to the dynamic viscosity as $[\nu = \frac{\mu}{\rho}]$. Substituting these on the equation 2.102 above yields

$$\frac{\partial \underline{q}}{\partial t} + (\underline{q}^T \cdot \underline{\nabla}) \underline{q} = \underline{f} - \frac{1}{\rho} \underline{\nabla} P + \nu (\underline{\nabla}^T \cdot \underline{\nabla} \underline{q}) \quad (2.103)$$

To introduce the second assumption to further simply the Navier - Stokes equations equations, we assume the fluid to be inviscid, which means that its viscosity is zero $\mu = 0$. With this assumption equation 2.103 takes the form

$$\frac{\partial \underline{q}}{\partial t} + (\underline{q}^T \cdot \underline{\nabla}) \underline{q} = \underline{f} - \frac{1}{\rho} \underline{\nabla} P \quad (2.104)$$

Equation 2.104 is the incompressible inviscid conservation of momentum expression and is also known as Euler equation.

We can obtain another useful form of the Euler equation by substituting the convective acceleration term $[(\underline{q}^T \cdot \nabla) \underline{q}]$, using the following vector identity

$$(\underline{q}^T \cdot \nabla) \underline{q} = \nabla \left(\frac{1}{2} \underline{q}^2 \right) - \underline{q} \times (\nabla \times \underline{q}) \quad (2.105)$$

For a derivation of the vector identity see Birk (2011).

Substituting the vector identity 2.105 in the Euler equation 2.104 we get

$$\frac{\partial \underline{q}}{\partial t} + \nabla \left(\frac{1}{2} \underline{q}^2 \right) - \underline{q} \times (\nabla \times \underline{q}) = f - \frac{1}{\rho} \nabla P \quad (2.106)$$

We will now introduce our last assumption in the re-arranged expression for the Euler equation 2.106. We will consider the flow to be irrotational. For irrotational flow the curl of the velocity is zero $[\nabla \times \underline{q} = 0]$. Thus, we obtain the Euler equation for irrotational flow

$$\frac{\partial \underline{q}}{\partial t} + \nabla \left(\frac{1}{2} \underline{q}^2 \right) = f - \frac{1}{\rho} \nabla P \quad (2.107)$$

We will use equation 2.107 to compute the pressure pressure in the fluid domain once we now the velocity.

We will find the velocity within the fluid domain using the continuity equation for incompressible flow 2.101, along with other assumptions (irrotational, incompressible), and characteristics of the flow that we will see in the next sections.

2.2.1 Potential Flows

With the Navier - Stokes equations and the continuity equation as starting point we proceeded to do the following assumptions:

1. We assumed the flow to be incompressible, which means that the density of the flow is constant
2. We assumed the flow to be inviscid, which means that the viscosity of the fluid is zero $\mu = 0$ and $\nu = \frac{\mu}{\rho} = 0$

3. We assumed the flow is irrotational i.e. $[curl(\underline{q}) = rot(\underline{q}) = (\nabla \times \underline{q}) = 0]$

With the above flow conditions incompressible, inviscid, and irrotational then a velocity potential exist in the flow.

Recall that by definition a potential is a scalar function that represents a conservative vector field. An example of a conservative vector field is a conservative force field like the gravity field. Conservative force fields have the physical characteristic consisting on that the work done to move from a point \underline{P}_0 to a point \underline{P}_1 is independent from the path we take to go from \underline{P}_0 to \underline{P}_1 .

In the case of the gravity field example of a conservative force field, we have that the potential of the gravity field is $[E = -gz]$, where g is the gravitational acceleration and z is the distance measured to the earth's center. Then, the work W per unit mass to move a body (neglecting the frictional effects which are not conservative) from a point $\underline{P}_0 = (x_0, y_0, z_0)$ to a point $\underline{P}_1 = (x_1, y_1, z_1)$ will be $W = E_1 - E_0 = -g(z_1 - z_0)$.

The sufficient condition for a vector field \underline{f} to be conservative and have a potential is to be irrotational i.e. $[curl(\underline{f}) = rot(\underline{f}) = (\nabla \times \underline{f}) = 0]$. This condition is also called integrability condition.

Additionally, $[curl(\underline{f}) = rot(\underline{f}) = (\nabla \times \underline{f}) = 0]$ only has to be enforced in simply connected regions.

Then, for an incompressible, inviscid flow, with no velocity rotation $[curl(\underline{q}) = rot(\underline{q}) = (\nabla \times \underline{q}) = 0]$ in a simply connected region, we can state that a velocity potential ϕ exist with $[\underline{q} = \nabla\phi]$

Now recall the circulation definition in equation 2.12

$$\Gamma = \oint_C \underline{q} \cdot d\underline{l} = \iint \zeta \cdot \underline{n} ds \quad (2.108)$$

We can state that the differential vorticity from the equation ?? above will takes the form

$$d\Gamma = udx + vdy + wdz \quad (2.109)$$

Substituting the velocity potential $[\nabla\phi = \underline{q}]$ in the differential vorticity equation 2.109 we get

$$d\Gamma = \frac{\partial\phi}{\partial x}dx + \frac{\partial\phi}{\partial y}dy + \frac{\partial\phi}{\partial z}dz = d\phi \quad ([\phi's] \text{ total differential}) \quad (2.110)$$

Then, if we take a potential flow (incompressible, inviscid, and irrotational) where by definition $[rot(\underline{q}) = (\nabla \times \underline{q}) = \underline{\zeta} = 0]$, and considering that $[\underline{n} \cdot d\underline{s} = d\underline{s}]$, we have that

$$\Gamma = \iint_s (\underline{\zeta})^T \cdot \underline{ds} = \iint_s (\underline{\nabla} \times \underline{q})^T \cdot \underline{ds} = \oint_c \underline{q}^T \cdot \underline{dl} = 0 \quad (2.111)$$

Then, we can additionally state from equation 2.110 that

$$\Gamma = \oint_c \underline{d\Gamma} = \oint_c \underline{d\phi} = \phi^- - \phi^+ = 0 \quad (2.112)$$

Equation 2.112 mean that the potential is single valued and helps us understand the integrability condition that is required for a vector field \underline{f} to be conservative, which is $[\underline{\nabla} \times \underline{f} = 0]$ enforced in a simply connected region.

2.2.2 The Laplace Equation

Recall the continuity equation again for incompressible flow

$$\underline{\nabla}^T \cdot (\underline{q}) = 0 \quad (2.113)$$

If in addition to incompressible, the flow is inviscid, and irrotational, then a velocity potential exist. Substituting the velocity potential $[\underline{\nabla}\phi = \underline{q}]$ in the continuity equation 2.113 we get

$$\underline{\nabla}^T (\underline{\nabla}\phi) = 0 \quad (2.114a)$$

$$(\underline{\nabla}^T \cdot \underline{\nabla}) \phi = 0 \quad (2.114b)$$

$$\underline{\nabla}^2 \phi = 0 \quad (2.114c)$$

$$\Delta \phi = 0 \quad (2.114d)$$

Equation 2.114d is called Laplace equation and we can write it in Cartesian coordinates as follows

$$\Delta \phi = \frac{\partial^2 \phi}{\partial x^2} + \frac{\partial^2 \phi}{\partial y^2} + \frac{\partial^2 \phi}{\partial z^2} = 0 \quad (2.115)$$

The Laplace equation 2.115 is a linear, partial, differential equation of second order. A solution of the Laplace equation yields the velocity potential $[\phi(x, y, z)]$ and subsequently the velocity field $[\underline{\nabla}\phi = \underline{q}]$.

2.2.3 Solving the Hydrodynamics Problem Using Potential Flow Theory

The hydrodynamics problem we are trying to solve using potential flow theory can have different scenarios. For instance, it can consist of a submerged body moving through a fluid with constant speed, for which we want to know the pressure distribution around the body. Other problem may include the interaction of a floating body with the free surface as it advances with constant speed and we want to know the resistance the body faces as it advances. A third variation of the two cases mentioned above is the hydrodynamic or aerodynamic lifting problem, consisting on calculating the lift generated by hydrofoil like bodies and the resistance to advance they find.

We will use potential flow theory to solve the problems described above, which are in essence, three variations of one single general problem. Recall that potential flow implies incompressible, inviscid and irrotational flow.

We will start by considering a deeply submerged body. Since we have a potential flow, we will use the continuity equation 2.113 expressed in terms of the velocity potential, or Laplace equation 2.114d to solve the problem

$$\underline{\nabla} \cdot \underline{q} = \underline{\nabla} \cdot (\underline{\nabla}\phi) = \Delta\phi = 0 \quad (2.116)$$

The Laplace equation $[\Delta\phi = 0]$ is an elliptical second order differential equation. In mathematical terms this implies that the state of the fluid at any position is influenced by the flow at all other positions. Thus, to solve the problem we will specify the values of the fluid quantities at the body boundary and the fluid domain boundary. After doing this we will be able to compute the fluid quantities anywhere in the fluid domain.

To specify the fluid quantities at the body surface, and fluid domain boundary, we will proceed as follows:

1. Body Boundary Condition. We will require no flow across the body boundary. We will write this mathematically as follows (considering a body fixed coordinate system)

$$\underline{\nabla}\phi \cdot \underline{n} = 0 \quad (\text{on the body surface}) S_b \quad (2.117)$$

2. Far field Boundary Condition. The boundary condition for the far field or boundary condition at infinity will require that the disturbance in the flow due to the body will vanish far away from the body. The boundary condition at infinity will take the form

$$\lim_{(r \rightarrow \infty)} \underline{\nabla}\phi = \underline{q} \quad (\text{on the far field}) S_\infty \quad (2.118)$$

2.2.4 General Solution of the Incompressible potential flow problem based in Green's Theorem

In the previous section we stated the basic potential flow problem in terms of the Laplace equation $[\Delta\phi = 0]$, and the two boundary conditions which are the boundary condition at infinity and the body boundary condition. In this section, we are going to use one of Green's theorems to derive a solution for the potential flow problem. Our approach will rather be general than detailed. For a complete treatment of the potential problem using Green's theorem see Birk (2011).

We will use the following form of Green's theorem to solve the hydrodynamics problem

$$\iint_s (\phi_1 \underline{\nabla} \phi_2 - \phi_2 \underline{\nabla} \phi_1)^T \cdot \underline{n} \, ds = \iiint_v \underline{\nabla}^T \cdot (\phi_1 \underline{\nabla} \phi_2 - \phi_2 \underline{\nabla} \phi_1) \, dv \quad (2.119)$$

In equation 2.119 the terms ϕ_1 and ϕ_2 are scalar functions of position. Additionally, the surface integral is taken over all surface boundaries S . These include the body boundary S_B , the boundary at infinity S_∞ , and when dealing with lifting surfaces the wake boundary S_W (see section 2.1.3).

If we expand the term inside of the volume integral we will get

$$\iint_s (\phi_1 \underline{\nabla} \phi_2 - \phi_2 \underline{\nabla} \phi_1)^T \cdot \underline{n} \, ds = \iiint_v (\phi_1 \underline{\nabla}^2 \phi_2 - \phi_2 \underline{\nabla}^2 \phi_1) \, dv \quad (2.120)$$

For the functions ϕ_1 and ϕ_2 we will peak $\phi_1 = \frac{1}{r}$ and for $\phi_2 = \phi$. It can be easily shown that both functions $[\phi_1 = \left(\frac{1}{r}\right)]$ and $[\phi_2 = \phi]$ satisfy the Laplace equation: $[\Delta \left(\frac{1}{r}\right) = \underline{\nabla}^2 \left(\frac{1}{r}\right) = 0]$ and $[\Delta(\phi) = \underline{\nabla}^2(\phi) = 0]$.

Note that r is the distance from a point $\underline{\aleph}$ in the body surface to an arbitrary point $(\underline{p}) = (x, y, z)$ on the fluid domain. Thus, for r we have

$$|r| = \|\underline{p} - \underline{\aleph}\| = \sqrt{(x - \aleph_x)^2 + (y - \aleph_y)^2 + (z - \aleph_z)^2} \quad (2.121)$$

Then, for $\left(\frac{1}{r}\right)$ we have

$$\left(\frac{1}{r}\right) = \frac{1}{\sqrt{(x - \aleph_x)^2 + (y - \aleph_y)^2 + (z - \aleph_z)^2}} \quad (2.122)$$

Now, after selecting the functions for $\phi_1 = \frac{1}{r}$, and $\phi_2 = \phi$, we can write the equation 2.120 for Green's theorem as follows

$$\iint_s \left[\left(\frac{1}{r} \right) \nabla \phi - \phi \nabla \left(\frac{1}{r} \right) \right]^T \cdot \underline{n} ds = \iiint_v \left[\left(\frac{1}{r} \right) \nabla^2 \phi - \phi \nabla^2 \left(\frac{1}{r} \right) \right] dv \quad (2.123)$$

When solving the integrals of Green's theorem on equation 2.123, we have to be careful. Note that the function $\frac{1}{r}$ will tend to infinity as the field point \underline{p} approaches the body point \underline{x} .

To find a solution for the Green's theorem equation we will evaluate three cases:

1. When the field point \underline{p} is outside the fluid domain V . In this case the function $\frac{1}{r}$ is bounded everywhere. Additionally, since the functions $\frac{1}{r}$ and ϕ both satisfy the Laplace equation then the volume integral will vanish

$$\iint_{S_B + S_\infty + S_W} \left[\left(\frac{1}{4\pi r} \right) \nabla \phi - \phi \nabla \left(\frac{1}{4\pi r} \right) \right]^T \cdot \underline{n} ds = 0 \quad \text{for } \underline{p} \notin [V] \quad (2.124)$$

2. The second case is when the field point \underline{p} is inside the fluid domain V . For this case we can not say anything about the volume integral because it may not exist. To solve this problem the point \underline{p} is excluded from the fluid domain by enclosing it in a small sphere with diameter ϵ . For a detailed derivation of this case see Birk (2011). Finally, the problem is solved by evaluating the surface integrals over each of the surfaces of the problem S_B , S_∞ , S_W , and the small sphere surface S_ϵ . The result of the integrations over the small sphere surface S_ϵ will yield

$$\iint_{S_\epsilon} \left[\left(\frac{1}{r} \right) \nabla \phi - \phi \nabla \left(\frac{1}{r} \right) \right]^T \cdot \underline{n} ds = -4\pi\phi(\underline{p}) \quad (2.125)$$

Consider that since we have excluded the point \underline{p} from the fluid domain, we have a similar condition to case 1 and the volume integral will vanish. Then, for the total surface integral we will get

$$\iint_{S_B + S_\infty + S_W} \left[\left(\frac{1}{4\pi r} \right) \nabla \phi - \phi \nabla \left(\frac{1}{4\pi r} \right) \right]^T \cdot \underline{n} ds = \phi(\underline{p}) \quad \text{for } \underline{p} \in [V] \quad (2.126)$$

3. The third case corresponds to when the field point \underline{p} is on the body surface S_B . For this case we apply a procedure similar to case 2. We enclose the point \underline{p} in a semi-sphere which will yield for the total surface integral the following result

$$\iint_{S_B+S_\infty+S_W} \left[\left(\frac{1}{4\pi r} \right) \nabla \phi - \phi \nabla \left(\frac{1}{4\pi r} \right) \right]^T \cdot \underline{n} \, ds = \frac{1}{2} \phi(\underline{p}) \quad \text{for } \underline{p} \in [S_B] \quad (2.127)$$

Recall that for the above examination of the integrals conforming the green's theorem expression, \underline{x} is a point on the body surface and \underline{p} is a field point that can be either out of the fluid domain (case 1 above), within the fluid domain (case 2), or on the body surface(case 3). We were considering the flow exterior to the body, and the body surface normal vector \underline{n} by convention was pointing out of the fluid domain (inside the body).

In our mathematical model the body boundary condition is $[\frac{\partial \phi}{\partial n} = 0 \text{ on } S_B]$, on a body fixed coordinate system, specifying no flow across the body surface. The body surface then becomes a stream function.

Regardless of the fact that we are interested in the exterior flow problem, let us consider the flow inside of the body. This flow will be described by the potential ϕ_i . If we evaluate a point \underline{p} outside of the interior flow domain V_i , we will recreate the first case (case 1) we had when dealing with Green's theorem for the exterior flow problem. The resulting integral after applying Green's theorem for the interior flow will be

$$\iint_{S_B} \left[\left(\frac{1}{4\pi r} \right) \nabla \phi_i - \phi_i \nabla \left(\frac{1}{4\pi r} \right) \right]^T \cdot \underline{n}_i \, ds = 0 \quad \text{for } \underline{p} \notin [V_i] \quad (2.128)$$

Note that in equation 2.128 the boundary consists of the body surface. Note that $\underline{n}_i = -\underline{n}$, thus we can replace the normal vector \underline{n}_i by the normal vector \underline{n} for the exterior flow domain V . Equation 2.128 will take the form

$$- \iint_{S_B} \left[\left(\frac{1}{4\pi r} \right) \nabla \phi_i - \phi_i \nabla \left(\frac{1}{4\pi r} \right) \right]^T \cdot \underline{n} \, ds = 0 \quad \text{for } \underline{p} \notin [V_i] \quad (2.129)$$

We can add equations 2.129 and 2.126 because both consider the point \underline{p} is located in the flow domain exterior to the body. Thus, we get:

$$\begin{aligned} \phi(\underline{p}) + 0 = & \iint_{S_B+S_\infty+S_W} \left[\left(\frac{1}{4\pi r} \right) \nabla \phi - \phi \nabla \left(\frac{1}{4\pi r} \right) \right]^T \cdot \underline{n} \, ds + \\ & - \iint_{S_B} \left[\left(\frac{1}{4\pi r} \right) \nabla \phi_i - \phi_i \nabla \left(\frac{1}{4\pi r} \right) \right]^T \cdot \underline{n} \, ds \quad \text{for } \underline{p} \in [V] \end{aligned} \quad (2.130a)$$

We can rewrite equation 2.130 as follows

$$\begin{aligned} \phi(\underline{p}) + 0 = & \iint_{S_\infty + S_W} \left[\left(\frac{1}{4\pi r} \right) \nabla \phi - \phi \nabla \left(\frac{1}{4\pi r} \right) \right]^T \cdot \underline{n} \, ds + \\ & \iint_{S_B} \left[\left(\frac{1}{4\pi r} \right) (\nabla \phi - \nabla \phi_i) - (\phi - \phi_i) \nabla \left(\frac{1}{4\pi r} \right) \right]^T \cdot \underline{n} \, ds \quad \text{for } \underline{p} \in [V] \end{aligned} \quad (2.131a)$$

The Far Field Potential [ϕ_∞]

We can evaluate the integrals of equation 2.131 over each surface separately. We can summarize the integral over the far field boundary surface S_∞ as the potential at infinity

$$\phi_\infty(\underline{p}) = \iint_{S_\infty} \left[\left(\frac{1}{4\pi r} \right) \nabla \phi - \phi \nabla \left(\frac{1}{4\pi r} \right) \right]^T \cdot \underline{n} \, ds \quad (2.132)$$

This is consistent with our physical model for the exterior flow problem. For a body moving at a constant speed \underline{q}_∞ the far field potential will be

$$\phi_\infty(\underline{p}) = -(u_\infty x + v_\infty y + w_\infty z) = -\underline{p}^T \cdot \underline{q}_\infty \quad (2.133)$$

The minus sign in the above equation is a matter of definition. An observer standing on the body moving with speed \underline{q}_∞ would see the water coming towards him. This is the reason for the minus sign. If we substitute the far field potential on our fluid flow equation 2.131, we get

$$\begin{aligned} \phi(\underline{p}) = & \iint_{S_W} \left[\left(\frac{1}{4\pi r} \right) \nabla \phi - \phi \nabla \left(\frac{1}{4\pi r} \right) \right]^T \cdot \underline{n} \, ds + \\ & \iint_{S_B} \left[\left(\frac{1}{4\pi r} \right) (\nabla \phi - \nabla \phi_i) - (\phi - \phi_i) \nabla \left(\frac{1}{4\pi r} \right) \right]^T \cdot \underline{n} \, ds + \phi_\infty(\underline{p}) \end{aligned} \quad (2.134a)$$

The Integral Over the Wake Surface [S_W]

For the integral over the wake surface S_W , we will assume the wake to be thin such that the velocity $\left[\frac{\partial \phi}{\partial n} \right]$, perpendicular to the wake is continuous across the wake.

Note that the wake is considered a barrier that transforms what would be a multiple connected region into a simply connected region, where a velocity potential can exist. See discussion on uniqueness of the solution Katz & Plotkin (2001) Section 2.8, and Birk (2011) Lecture 8.

In the following equations ϕ^- indicates the value of the velocity potential ϕ in the b^- side of the wake or barrier. See figure [Wake barrier]. ϕ^+ indicates the value of the velocity potential ϕ in the b^+ side of the wake or barrier.

In the wake the normal derivative of the velocity potential $\frac{\partial\phi}{\partial n}$ has to be continuous across the barrier, which means the normal velocity is continuous across the barrier. This because the continuity equation prohibits jumps in velocity. Additionally, since there is no jump in velocity the wake won't be taking any hydrodynamic loads. Then, we have

$$\frac{\partial\phi^-}{\partial n} = \frac{\partial\phi^+}{\partial n} = \frac{\partial\phi}{\partial n}, \quad \left(\text{because } \frac{\partial\phi}{\partial n} \text{ is continuous across the barrier} \right) \quad (2.135)$$

Now, if we analyse the surface integral over the wake in equation 2.134, we will get

$$\begin{aligned} & \iint_{S_w} \left[\left(\frac{1}{4\pi r} \right) \nabla \phi - \phi \nabla \left(\frac{1}{4\pi r} \right) \right]^T \cdot \underline{n} \, ds = \\ & \left(\frac{1}{4\pi} \right) \left[\iint_{b^-} \left(\frac{1}{r} \right) (\nabla\phi^-)^T \cdot \underline{n} \, ds - \iint_{b^+} \left(\frac{1}{r} \right) (\nabla\phi^+)^T \cdot \underline{n} \, ds \right] + \\ & - \left(\frac{1}{4\pi} \right) \left[\iint_{b^-} \phi^- \left(\nabla \left(\frac{1}{r} \right) \right)^T \cdot \underline{n} \, ds - \iint_{b^+} \phi^+ \left(\nabla \left(\frac{1}{r} \right) \right)^T \cdot \underline{n} \, ds \right] \end{aligned} \quad (2.136)$$

Recall that we are considering the wake to be very thin. Additionally, if we factor terms the above equation yields

$$\left(\frac{1}{4\pi} \right) \left[\iint_b \left(\frac{1}{r} \right) \left(\frac{\partial\phi^-}{\partial n} - \frac{\partial\phi^+}{\partial n} \right) ds \right] - \left(\frac{1}{4\pi} \right) \left[\iint_b (\phi^- - \phi^+) \left(\nabla \left(\frac{1}{r} \right) \right)^T \cdot \underline{n} \, ds \right] \quad (2.137)$$

Note that in equation 2.137, the first integral will vanish because $\left[\frac{\partial\phi^-}{\partial n} = \frac{\partial\phi^+}{\partial n} \right]$. As a result, we will get for the integral over the wake surface

$$\iint_{S_w} \left[\left(\frac{1}{4\pi r} \right) \nabla \phi - \phi \nabla \left(\frac{1}{4\pi r} \right) \right]^T \cdot \underline{n} \, ds = \left(\frac{1}{4\pi} \right) \left[\iint_b (\phi^- - \phi^+) \left(\nabla \left(\frac{1}{r} \right) \right)^T \cdot \underline{n} \, ds \right] \quad (2.138)$$

Note that in equation 2.138, the letter [b] stands for barrier, meaning that we are taking the integral over the barrier surface which is the same as the wake.

Final Equation Obtained from Green's Theorem Applied to the Potential Flow Problem

We have worked out the integrals over the far field surface and the wake surface introducing some assumptions related to the physical characteristics of the fluid flow problem.

Now we can write equation 2.134 as follows

$$\begin{aligned} \phi(\underline{p}) = & \iint_{S_B} \left[\left(\frac{1}{4\pi r} \right) (\nabla \phi - \nabla \phi_i) - (\phi - \phi_i) \nabla \left(\frac{1}{4\pi r} \right) \right]^T \cdot \underline{n} \, ds + \\ & \left(\frac{1}{4\pi} \right) \left[\iint_{S_w} (\phi^- - \phi^+) \left(\nabla \left(\frac{1}{r} \right) \right)^T \cdot \underline{n} \, ds \right] + \phi_\infty(\underline{p}) \quad (2.139a) \end{aligned}$$

Now, if we substitute $[\nabla \cdot \underline{n} = \frac{\partial()}{\partial \underline{n}}]$ in the equation 2.139 above, we get

$$\begin{aligned} \phi(\underline{p}) = & \iint_{S_B} \left[\left(\frac{1}{4\pi r} \right) \left(\frac{\partial \phi}{\partial \underline{n}} - \frac{\partial \phi_i}{\partial \underline{n}} \right) - (\phi - \phi_i) \frac{\partial}{\partial \underline{n}} \left(\frac{1}{4\pi r} \right) \right] ds + \\ & \left(\frac{1}{4\pi} \right) \left[\iint_{S_w} (\phi^- - \phi^+) \left(\frac{\partial}{\partial \underline{n}} \left(\frac{1}{r} \right) \right) ds \right] + \phi_\infty(\underline{p}) \quad (2.140a) \end{aligned}$$

For the terms in equation 2.140 we can define

$$\begin{aligned} -\sigma &= \left(\frac{\partial \phi}{\partial \underline{n}} - \frac{\partial \phi_i}{\partial \underline{n}} \right) \\ -\mu &= (\phi - \phi_i) \end{aligned} \quad (2.141)$$

Where σ is the yet unknown source strength, and μ is the yet unknown double strength. Note that for the wake S_w the doublet strength is $-\mu = \phi^+ - \phi^-$ which is the difference between the potential in the upper and lower surface of the barrier b or wake.

Finally, our integral equation derived based on green's theorem will take the form

$$\begin{aligned} \phi(\underline{p}) = & \iint_{S_B} \left[\left(\sigma \frac{-1}{4\pi r} \right) - \mu \left(\frac{\partial}{\partial n} \left(\frac{-1}{4\pi r} \right) \right) \right] ds \\ & + \left(\frac{1}{4\pi} \right) \iint_{S_w} \mu \left(\frac{\partial}{\partial n} \left(\frac{1}{r} \right) \right) ds + \phi_\infty(\underline{p}) \end{aligned} \quad (2.142)$$

For the purpose of visualization we can reorganize the terms in the equation as follows

$$\begin{aligned} \phi(\underline{p}) = & \left(\frac{-1}{4\pi} \right) \iint_{S_B} \sigma \left(\frac{1}{r} \right) ds + \frac{1}{4\pi} \iint_{S_B} \mu \left(\frac{\partial}{\partial n} \left(\frac{1}{r} \right) \right) ds \\ & + \left(\frac{1}{4\pi} \right) \iint_{S_w} \mu \left(\frac{\partial}{\partial n} \left(\frac{1}{r} \right) \right) ds + \phi_\infty(\underline{p}) \end{aligned} \quad (2.143)$$

2.2.5 Solution of the Boundary Value Problem for the Flow Around a Fully Submerged Body

We have derived the equation 2.143 based on Green's Theorem. This equations is a general expression for the velocity potential.

In order to find a solution for the flow around a fully submerged body, we will need to combine equation 2.143 with the boundary condition that characterize our problem.

In the following equations we will change the notation as follows. The field point will be \underline{p} , which is were we will compute the induced potential or velocity. The influence point will be \underline{q} . The velocity at which the body (hydrofoil or ship) is travelling or moving will be called \underline{U}_b . Also, note that for a body fixed coordinate system $\underline{U}_b = \underline{v}_\infty$, where \underline{v}_∞ is the velocity at infinity or far field velocity.

For the solution of the fully submerged body we will use the following boundary conditions:

1. The body Boundary Condition. This condition requires no flow across the body surface. We can write this mathematically for a body fixed coordinate system as follows

$$\frac{\partial \phi}{\partial \underline{n}} = 0, \quad \text{on } S_b \quad (2.144)$$

2. The Far Field Boundary Condition. This condition requires that the disturbance due to the body on the fluid domain will vanish far away from the body. Mathematically we write

$$\lim_{(\underline{r} \rightarrow \infty)} \underline{\nabla} \phi = \underline{v}_\infty = \underline{U}_b \quad (\text{on the far field}) S_\infty \quad (2.145)$$

Note that equation 2.143 satisfies the far field boundary condition automatically. Substituting the potential from equation 2.143 in the equation 2.145 we get

$$\begin{aligned} & \lim_{(\underline{r} \rightarrow \infty)} \underline{\nabla} \phi = \\ & \underline{\nabla} \left(\left(\frac{-1}{4\pi} \right) \iint_{S_B} \sigma \left(\frac{1}{\underline{r}} \right) ds + \frac{1}{4\pi} \iint_{S_B} \mu \left(\frac{\partial}{\partial \underline{n}} \left(\frac{1}{\underline{r}} \right) \right) ds + \left(\frac{1}{4\pi} \right) \iint_{S_W} \mu \left(\frac{\partial}{\partial \underline{n}} \left(\frac{1}{\underline{r}} \right) \right) ds + \phi_\infty(\underline{p}) \right) \end{aligned} \quad (2.146)$$

In equation 2.146 the integrals containing the term $\frac{1}{\underline{r}}$ will vanish for $\underline{r} \rightarrow \infty$, leaving only $\underline{\nabla} \phi_\infty$, which is the definition of ϕ_∞ . See 2.2.4 for the definition and physical interpretation of the far field potential.

Now, if we substitute the potential from equation 2.143 into the equation 2.144 for the body boundary condition, we will get the equation below:

$$\begin{aligned} & \frac{\partial}{\partial \underline{n}} \left(\left(\frac{-1}{4\pi} \right) \iint_{S_B} \sigma(\underline{q}) \left(\frac{1}{r(\underline{p}, \underline{q})} \right) ds(\underline{q}) \right) + \frac{\partial}{\partial \underline{n}} \left(\frac{1}{4\pi} \iint_{S_B} \mu(\underline{q}) \left(\frac{\partial}{\partial \underline{n}} \left(\frac{1}{r(\underline{p}, \underline{q})} \right) \right) ds(\underline{q}) \right) \\ & + \frac{\partial}{\partial \underline{n}} \left(\left(\frac{1}{4\pi} \right) \iint_{S_W} \mu(\underline{q}) \left(\frac{\partial}{\partial \underline{n}} \left(\frac{1}{r(\underline{p}, \underline{q})} \right) \right) ds(\underline{q}) \right) + \frac{\partial}{\partial \underline{n}} (\phi_\infty(\underline{p})) = 0 \end{aligned} \quad (2.147)$$

On equation 2.147 for the body boundary condition, we are enforcing the boundary condition at a point \underline{p} on the body surface. Recall that the body boundary condition requires no flow across the body surface $\frac{\partial \phi}{\partial \underline{n}} = 0$. Thus, the normal derivative uses the body surface normal vector at

point \underline{p} and the gradient at this point. Recall that $\frac{\partial}{\partial \underline{n}} = \underline{n}_p^T \nabla_p$.

Additionally, note that the normal derivative operator is independent of the integration variable and we may interchange derivation and integration. Then, equation 2.147 would take the form

$$\begin{aligned} & \left(\frac{-1}{4\pi} \right) \iint_{S_B} \sigma(\underline{q}) \underline{n}_p^T \cdot \nabla_p \left(\frac{1}{r(\underline{p}, \underline{q})} \right) ds(\underline{q}) + \frac{1}{4\pi} \iint_{S_B} \mu(\underline{q}) \underline{n}_p^T \cdot \nabla_p \left(\frac{\partial}{\partial \underline{n}} \left(\frac{1}{r(\underline{p}, \underline{q})} \right) \right) ds(\underline{q}) \\ & + \left(\frac{1}{4\pi} \right) \iint_{S_W} \mu(\underline{q}) \underline{n}_p^T \cdot \nabla_p \left(\frac{\partial}{\partial \underline{n}} \left(\frac{1}{r(\underline{p}, \underline{q})} \right) \right) ds(\underline{q}) + \underline{n}_p^T \cdot \nabla_p (\phi_\infty(\underline{p})) = 0 \end{aligned} \quad (2.148)$$

Note that in equation 2.148, in the integrals corresponding to the body surface, we will have to compute what is called a principal value integral, in order to deal with the singularity that occurs when $\underline{p} = \underline{q}$. The result of computing the principal value integral for the sources is $-\frac{1}{2}\sigma(\underline{p}) = -\frac{1}{2}\sigma(\underline{q})$. The physical interpretation of this result is that the effect (which in this case the perpendicular velocity) induced by a source point on it self i.e $\underline{p} = \underline{q}$, is equal to one half of the source strength. For a detailed derivation of the computation of the principal value integral see Birk (2011) Lecture 10.

Dealing with the singularity case when $\underline{p} = \underline{q}$ is more cumbersome for dipole elements. In Chapter no. 3, we will observe that the analytical expressions we will use to compute the dipole induced velocity will not present a singularity when $\underline{p} = \underline{q}$. The formulae we are going to use were introduced by Hess and Smith (1972). See Hess (1972)

After computing the principal value for the integrals over the body surface, the equation will take the form

$$\begin{aligned} & -\frac{1}{2}\sigma(\underline{p}) + \left(\frac{-1}{4\pi} \right) \iint_{S_B} \sigma(\underline{q}) \underline{n}_p^T \cdot \nabla_p \left(\frac{1}{r(\underline{p}, \underline{q})} \right) ds(\underline{q}) \\ & + \frac{1}{4\pi} \iint_{S_B} \mu(\underline{q}) \underline{n}_p^T \cdot \nabla_p \left(\frac{\partial}{\partial \underline{n}} \left(\frac{1}{r(\underline{p}, \underline{q})} \right) \right) ds(\underline{q}) \\ & + \left(\frac{1}{4\pi} \right) \iint_{S_W} \mu(\underline{q}) \underline{n}_p^T \cdot \nabla_p \left(\frac{\partial}{\partial \underline{n}} \left(\frac{1}{r(\underline{p}, \underline{q})} \right) \right) ds(\underline{q}) + \underline{n}_p^T \cdot \nabla_p (\phi_\infty(\underline{p})) = 0 \end{aligned} \quad (2.149)$$

Note that the integral for the body sources, is valid for all body points except when $\underline{p} = \underline{q}$, in which case the influence of a source point on itself is $-\frac{1}{2}\sigma(\underline{p})$

Chapter 3

Computational Implementation of Flows with Free Surface

3.1 Basic Integral Equation to Describe the Problem

To solve the hydrodynamic lifting problem using potential flow, we will employ a modified version of equation 2.149. In our new equation we have to include the free surface as a new integration surface. Additionally, we will have to satisfy a boundary condition on the free surface.

Note that, as we stated in the final part of the previous chapter, we will change the notation in the equations that follow. The field point will be \underline{p} , which is where we will compute the induced potential or velocity. The influence point will be \underline{q} . The velocity at which the body (hydrofoil or ship) is travelling or moving will be called \underline{U}_b . Also, note that for a body fixed coordinate system $\underline{U}_b = \underline{v}_\infty$, where \underline{v}_∞ is the velocity at infinity or far field velocity.

Let us state the boundary conditions we have to satisfy for our fluid flow problem in the presence of the free surface:

1. The body Boundary Condition. This condition requires no flow across the body surface. We can write this mathematically for a body fixed coordinate system as follows

$$\frac{\partial \phi}{\partial \underline{n}} = 0, \quad \text{on } S_b \quad (3.1)$$

2. The Far Field Boundary Condition. This condition requires that the disturbance due to the body on the fluid domain will vanish far away from the body. Mathematically we write

$$\lim_{(r \rightarrow \infty)} \nabla \phi = \underline{v}_\infty = \underline{U}_b \quad (\text{on the far field}) S_\infty \quad (3.2)$$

3. The Free Surface Boundary Condition. This boundary condition is divided in two parts.

- (a) The Kinematic Free Surface Boundary Condition. Here we will require that no flow particle is allowed to pass through the free surface. This condition turns the free surface into a stream surface like the body surface. We express this mathematically as follows

$$\frac{\partial\phi}{\partial\mathbf{n}} = \mathbf{n}^T \cdot (\nabla\phi) = 0, \quad \text{at } z = \zeta(x, y) \quad (3.3)$$

Where $z = \zeta(x, y)$ is an implicit function describing the yet unknown shape of the free surface. The equation for the kinematic free surface boundary condition can be further expanded expressing the normal vector in terms of the gradient. See Birk (2011) for details and derivation of equations.

$$-\zeta_x\phi_x - \zeta_y\phi_y + \phi_z = 0 \quad \text{on } z = \zeta(x, y) \quad (3.4)$$

In equation 3.4 the sub-indexes denote differentiation in a specific direction e.g. ϕ_x means the derivative of the potential ϕ in the x - *direction*. Note that the condition in equation 3.4 is non linear because it presents products of unknown quantities.

We can linearize the above equation for the kinematic free surface boundary condition applying a perturbation method. Then, the resulting equation can be even further simplified applying the Neumann-Kelvin Linearization approach, which consists on assuming a basic solution for both the velocity potential and the wave field. For the solution, the first order potential will be taken to be equal to be the potential of the velocity at infinity (parallel flow) $\phi^{(0)} = -U_b x$, and no waves will be assume as base solution $\zeta^{(0)} = 0$ for the free surface.

Using the described linearization process the linearized free surface kinematic boundary condition will take the form:

$$-\zeta_x^{(1)}(-U_b) + \phi_z^{(1)} = 0 \quad \text{on } z = 0 \quad (3.5)$$

where the $\phi^{(1)}$ is the first order potential, and $\zeta^{(1)}$ is the first order wave elevation. The parallel flow assumption implies that the disturbance in the flow field due to the body is represented by the first order potential. For a detailed derivation of the kinematic boundary condition and its linearization please see Lectures 15, 16, and 17 of Birk (2011).

- (b) The Free Surface Dynamic Boundary Condition. This condition states that the pressure at all points on the free surface is equal to the air pressure. To express this condition mathematically we use Bernoulli's equation. Using a body fixed coordinate system, the equation will take the form

$$P_\infty + \rho gz + \frac{1}{2}\rho[\nabla\phi]^2 = P_\infty + \frac{1}{2}\rho U_b^2 \quad \text{on } z = \zeta(x, y) \quad (3.6)$$

The dynamic boundary condition is also non-linear. To linearize the dynamic boundary condition we employ the same procedure used for the kinematic boundary condition. First, we employ the perturbation method, and then we use the Neumann - Kelvin linearizaion approach. This process results in the following expression

$$U_b \phi_x^{(1)} - g \zeta^{(1)} = 0 \quad \text{on} \quad z = 0 \quad (3.7)$$

For the solution of our problem we will use a boundary condition for the free surface that combines both the linearized kinematic boundary condition and the linearized dynamic boundary condition. This expression will take the form

$$U_b^2 \phi_{xx}^{(1)} + g \phi_z^{(1)} = 0 \quad \text{on} \quad z = 0 \quad (3.8)$$

In the previous chapter we derived the basic equation 2.149 that describe the problem for a fully submerged body. As we stated before, we can expand this equation to include the new boundary condition for the free surface as follows

$$\begin{aligned}
& - \frac{1}{2} \sigma(\underline{p}) + \underline{n}_p^T \iint_{S_{f'}+S_b} \sigma(\underline{q}) \nabla_p \left(\frac{-1}{4\pi r(\underline{p}, \underline{q})} \right) ds_q \\
& - \iint_{S_b} \mu(\underline{q}) \nabla \left[\frac{\partial}{\partial \underline{n}} \left(\frac{-1}{4\pi r(\underline{p}, \underline{q})} \right) \right] ds_q \\
& - \iint_{S_w} \mu(\underline{q}) \nabla \left[\frac{\partial}{\partial \underline{n}} \left(\frac{-1}{4\pi r(\underline{p}, \underline{q})} \right) \right] ds_q = \underline{n}^T \cdot U_b \quad , \quad \text{for} \quad \underline{p} \in S_b \\
& + U_b^2 \iint_{S_{f'}+S_b} \sigma(\underline{q}) \frac{\partial^2}{\partial x^2} \left(\frac{-1}{4\pi r(\underline{p}, \underline{q})} \right) ds_q + g \iint_{S_{f'}+S_b} \sigma(\underline{q}) \frac{\partial}{\partial z} \left(\frac{-1}{4\pi r(\underline{p}, \underline{q})} \right) ds_q \\
& - U_b^2 \iint_{S_b} \mu(\underline{q}) \frac{\partial^2}{\partial x^2} \left[\frac{\partial}{\partial \underline{n}} \left(\frac{-1}{4\pi r(\underline{p}, \underline{q})} \right) \right] ds_q - g \iint_{S_b} \mu(\underline{q}) \frac{\partial}{\partial z} \left[\frac{\partial}{\partial \underline{n}} \left(\frac{-1}{4\pi r(\underline{p}, \underline{q})} \right) \right] ds_q \\
& + U_b^2 \iint_{S_w} \mu(\underline{q}) \frac{\partial^2}{\partial x^2} \left[\frac{\partial}{\partial \underline{n}} \left(\frac{1}{4\pi r(\underline{p}, \underline{q})} \right) \right] ds_q \\
& + g \iint_{S_w} \mu(\underline{q}) \frac{\partial}{\partial z} \left[\frac{\partial}{\partial \underline{n}} \left(\frac{1}{4\pi r(\underline{p}, \underline{q})} \right) \right] ds_q = 0 \quad , \quad \text{for} \quad \underline{p} \in S_f \quad z = 0
\end{aligned} \quad (3.9)$$

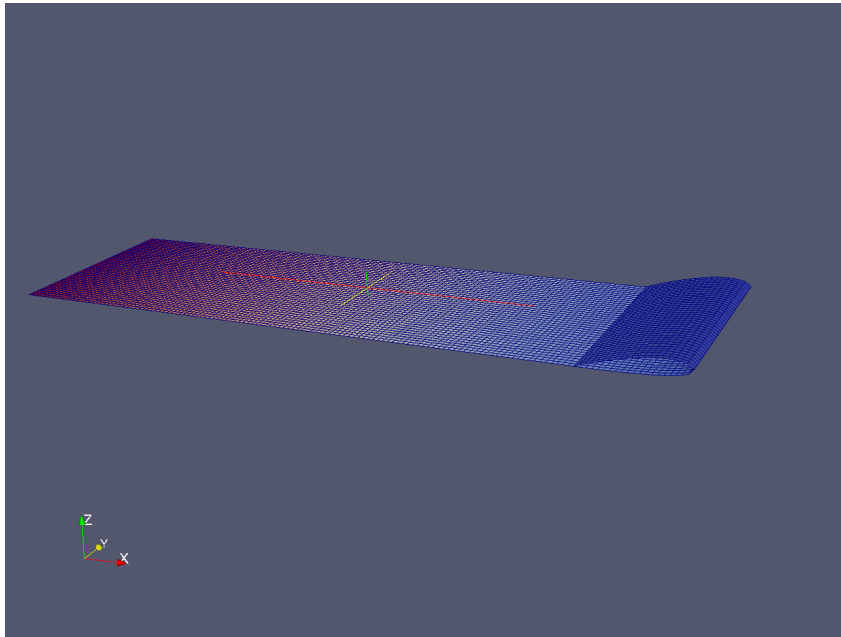


Figure 3.1: Foil geometry discretization NACA2415

3.2 Discretization of Basic Integral Equation

To solve the equation 3.9, we will discretize the surfaces of the fluid domain where we are enforcing the boundary conditions. Also, this discretization will help us to compute the integrals over these surfaces.

Basically, the body surface and the free surface are composed by an infinite number of points, then, the boundary conditions on the body surface S_b and the free surface S_f , have to be satisfied at an infinite number of points. Additionally, to perform the integration, the unknown source strength σ , and the unknown dipole strength μ , are part of the integrals.

To solve the integration problem we will discretize the body surface and the free surface in a finite number of quadrilateral panels. By doing this we can assume some local distribution of the singularities σ and μ over the panels, and we can take them out of the integral.

We will also use the discretization of the body surface and the free surface, so that we will enforce the boundary condition in the center points of the panels. See figure 3.1 for the discretization of a fully submerged foil; and figure 3.2 for a submerged foil close to the free surface.

We should note that by increasing the number of panels, we will model better the body geometry and the free surface; and if we use an infinite number of panels we will model the exact body

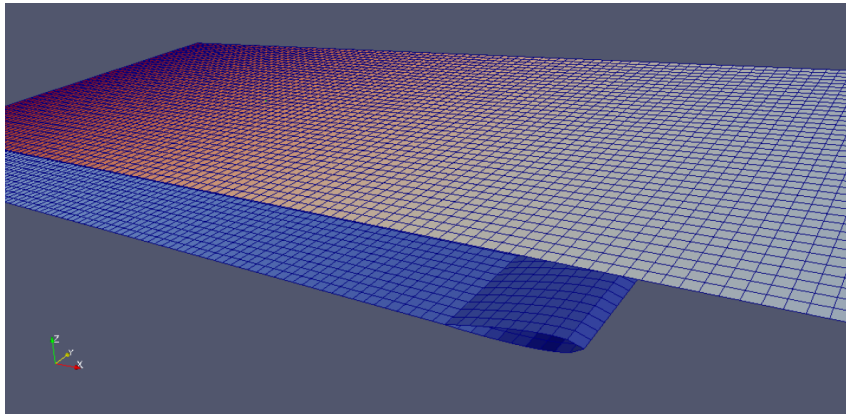


Figure 3.2: NACA2415 Foil geometry discretization with free surface. Foil Submerged 0.5 chord lengths

geometry, and the exact free surface shape or wave field.

Additionally, consider that we will be enforcing the body boundary condition at the center of each panel, thus, there will only be no flow across the body surface at the panels centers. This is another reason why, the flow problem modeling will get more accurate by increasing the number of panels. Note that this also applies to the free surface.

The discretized equation will take the form

$$\begin{aligned}
& -\frac{1}{2}\sigma(\underline{p}_i) + \sum_{j=1}^{N_b+N_f} \sigma(\underline{q}_j) \underline{n}_{p_i}^T \iint_{S_{f'}+S_b} \nabla_{p_i} \left(\frac{-1}{4\pi r(\underline{p}_i, \underline{q}_j)} \right) ds_{q_j} \\
& - \sum_{j=1}^{N_b} \mu(\underline{q}_j) \iint_{S_b} \nabla \left[\frac{\partial}{\partial \underline{n}} \left(\frac{-1}{4\pi r(\underline{p}_i, \underline{q}_j)} \right) \right] ds_{q_j} \\
& - \sum_{j=1}^{N_w} \mu(\underline{q}_j) \iint_{S_w} \nabla \left[\frac{\partial}{\partial \underline{n}} \left(\frac{-1}{4\pi r(\underline{p}_i, \underline{q}_j)} \right) \right] ds_{q_j} = \underline{n}(\underline{p}_i)^T \cdot \underline{U}_b
\end{aligned}$$

with $\underline{p}_i \in S_b$ and $i = 1, 2, \dots, N_b$

$$\begin{aligned}
& + U_b^2 \sum_{j=1}^{N_b+N_f} \sigma(\underline{q}_j) \iint_{S_{f'}+S_b} \frac{\partial^2}{\partial x^2} \left(\frac{-1}{4\pi r(\underline{p}_i, \underline{q}_j)} \right) ds_{q_j} \\
& + g \sum_{j=1}^{N_b+N_f} \sigma(\underline{q}_j) \iint_{S_{f'}+S_b} \frac{\partial}{\partial z} \left(\frac{-1}{4\pi r(\underline{p}_i, \underline{q}_j)} \right) ds_{q_j} \\
& - U_b^2 \sum_{j=1}^{N_b} \mu(\underline{q}_j) \iint_{S_b} \frac{\partial^2}{\partial x^2} \left[\frac{\partial}{\partial \underline{n}} \left(\frac{-1}{4\pi r(\underline{p}_i, \underline{q}_j)} \right) \right] ds_{q_j} \\
& - g \sum_{j=1}^{N_b} \mu(\underline{q}_j) \iint_{S_b} \frac{\partial}{\partial z} \left[\frac{\partial}{\partial \underline{n}} \left(\frac{-1}{4\pi r(\underline{p}_i, \underline{q}_j)} \right) \right] ds_{q_j} \\
& + U_b^2 \sum_{j=1}^{N_b} \mu(\underline{q}_j) \iint_{S_w} \frac{\partial^2}{\partial x^2} \left[\frac{\partial}{\partial \underline{n}} \left(\frac{-1}{4\pi r(\underline{p}_i, \underline{q}_j)} \right) \right] ds_{q_j} \\
& + g \sum_{j=1}^{N_b} \mu(\underline{q}_j) \iint_{S_w} \frac{\partial}{\partial z} \left[\frac{\partial}{\partial \underline{n}} \left(\frac{-1}{4\pi r(\underline{p}_i, \underline{q}_j)} \right) \right] ds_{q_j} = 0
\end{aligned}$$

where \underline{q} is above S_f with $\underline{p}_i \in S_f$ at $z = 0$ and $i = N_b + 1, N_b + 2, \dots, N_b + N_f$

(3.10)

3.3 Building the Numerical Solution

As indicated in the equations 3.10, we will build the numerical solution for our flow problem by distributing a finite number of singularities over the body surface and the free surface of the fluid domain.

For fully submerged bodies, we will use a distribution of sources and a distribution of dipoles over the body surface. The dipoles and the sources will interact as part of the solution of the lifting problem. For problems that does not include lifting, a source distribution can be used to solve the so called body thickness problem. For problems involving lifting and circulation, it is necessary to use a singularity such as vortices or dipoles.

In the previous chapters we derived the potentials induced at a point p in the fluid domain, by a source distribution and a dipole distribution. Now, for completeness, we write the expressions again. The potential induced by a point $\underline{q}^T = (x_0, y_0, z_0)$ at a point $\underline{p}^T = (x, y, z)$ on the fluid domain will take the form

$$\phi(x, y, z) = \frac{-\sigma}{4\pi\sqrt{(x-x_0)^2 + (y-y_0)^2 + (z-z_0)^2}} \quad (3.11)$$

The velocities induced at the point \underline{p} by the source located at a point \underline{q} can be found by taking the gradient of the velocity potential

$$u(x, y, z) = \frac{\partial\phi}{\partial x} = \frac{\sigma(x-x_0)}{4\pi[(x-x_0)^2 + (y-y_0)^2 + (z-z_0)^2]^{3/2}} \quad (3.12)$$

$$v(x, y, z) = \frac{\partial\phi}{\partial y} = \frac{\sigma(y-y_0)}{4\pi[(x-x_0)^2 + (y-y_0)^2 + (z-z_0)^2]^{3/2}} \quad (3.13)$$

$$z(x, y, z) = \frac{\partial\phi}{\partial z} = \frac{\sigma(z-z_0)}{4\pi[(x-x_0)^2 + (y-y_0)^2 + (z-z_0)^2]^{3/2}} \quad (3.14)$$

The potential induced at a point p by a doublet located at point q will take the form

$$\phi(x, y, z) = \frac{\mu}{4\pi} (\nabla) \left(\frac{1}{\sqrt{(x-x_0)^2 + (y-y_0)^2 + (z-z_0)^2}} \right) \quad (3.15)$$

Note that we have to take the gradient of the term $\frac{1}{r}$ to find the doublet induced potential. We will take the derivative in the direction in which the doublet axis is directed. For instance, for a doublet which axis is directed in the z – *direction* the doublet induced potential will be

$$\phi(x, y, z) = \frac{-\mu}{4\pi} (z - z_0) [(x - x_0)^2 + (y - y_0)^2 + (z - z_0)^2]^{3/2} \quad (3.16)$$

For our implementation we will use an equivalent expression to equation 3.16, which is the potential induced at a point \underline{p} on the fluid domain, by a dipole oriented in the z – *direction*, located at a point $q^T(x_0, y_0, z_0)$. We will apply a similar expression to this formula because in each of the panels of the body surface (and all surfaces with a dipole distribution), the dipoles will point perpendicular to the body surface in the z – *direction* of the local panel coordinate system. Never the less, it is important to note that equation 3.16, refers to the influence of a point dipole; and for our program we will use a constant dipole distribution over each the panel. The same applies to the sources, we will use a constant source distribution over each source panel.

First Order panel Method

We will use first order panels, which implies that the singularities will be constantly distributed over the panels. For first order panels the expression for the velocity potential induced by the singularities will change, as compared to the ones showed above. Hess & Smith derived the expression for the induced potential, as well as the induced velocities, for panels with a constant sources distribution, and for panels with a constant dipole distribution. See (Hess & Smith, 1964; Newman, 1986) for the corresponding formulae. These formulae were used in our program.

In the following section we will present the exact formulae used to compute the induced potential, the induced velocities, and the second order derivatives of the potential for both, a panel with a constant strength source distribution, and a panel with a constant strength dipole distribution. The equations on the next section will be used to compute the influence coefficients for the system of linear equations that represents the discretized integral equation.

3.3.1 Exact formulas

In the summations below the index k takes values from 1 through 4 representing the number of a panel edge or corner. In case $k = 4$ the value of $k + 1 = 5$ is set to $k + 1 := 1$.

All coordinates are with respect to the coordinate system local to the planar quadrilateral panel. The origin of the local panel coordinate system is located at the panel center, with the x –axis pointing from the middle of edge 4 (between point 4 and 1) through the middle of edge 2 (between points 2 and 3). The y –axis is perpendicular to the x – *axis* in the panel plane, and

the z -axis is normal to the x -axis and the y -axis. x, y, z form a righthanded Cartesian coordinate system.

$(x, y, z)^T$ point where we evaluate potential derivatives (fieldpoint or collocation point)

$(x_k, y_k)^T$ coordinates of panel corners $k = 1, 2, 3, 4$; $z_k = 0$ in panel plane

$$d_k = \sqrt{(x_{k+1} - x_k)^2 + (y_{k+1} - y_k)^2} \quad \text{length of panel edge } k \quad (3.17)$$

$$e_k = (x - x_k)^2 + z^2 \quad (3.18)$$

$$h_k = (x - x_k)(y - y_k) \quad (3.19)$$

$$m_k = \frac{(y_{k+1} - y_k)}{(x_{k+1} - x_k)} \quad \text{tangens of angle between } x\text{-axis and edge } k \quad (3.20)$$

$$r_k = \sqrt{(x - x_k)^2 + (y - y_k)^2 + z^2} \quad \text{distance between panel corner } k \text{ and fieldpoint} \quad (3.21)$$

For some of the second order derivatives we also use the following abbreviations to shorten the presented equations.

$$\varrho_k = \left[r_k r_{k+1} + (x - x_k)(x - x_{k+1}) + (y - y_k)(y - y_{k+1}) + z^2 \right] \quad (3.22)$$

$$\lambda_k = \left[(x - x_k)(y - y_{k+1}) - (x - x_{k+1})(y - y_k) \right] \quad (3.23)$$

Velocity potential for source distribution

$$\Phi = \sigma \cdot \phi \quad (3.24)$$

$$\begin{aligned} \phi = \frac{-1}{4\pi} \sum_{k=1}^4 \left\{ \left(\frac{(x - x_k)(y_{k+1} - y_k) - (y - y_k)(x_{k+1} - x_k)}{d_k} \right) \cdot \ln \left(\frac{r_k + r_{k+1} - d_k}{r_k + r_{k+1} + d_k} \right) \right. \\ \left. + z \left[\tan^{-1} \left(\frac{m_k e_k - h_k}{z r_k} \right) - \tan^{-1} \left(\frac{m_k e_{k+1} - h_{k+1}}{z r_{k+1}} \right) \right] \right\} \quad (3.25) \end{aligned}$$

Velocities induced by source distribution

$$\begin{aligned}
 \phi_x &= \frac{\partial \phi}{\partial x} \\
 &= \frac{-1}{4\pi} \sum_{k=1}^4 \frac{y_{k+1} - y_k}{d_k} \cdot \ln \left(\frac{r_k + r_{k+1} - d_k}{r_k + r_{k+1} + d_k} \right)
 \end{aligned} \tag{3.26}$$

$$\begin{aligned}
 \phi_y &= \frac{\partial \phi}{\partial y} \\
 &= \frac{-1}{4\pi} \sum_{k=1}^4 \frac{-(x_{k+1} - x_k)}{d_k} \cdot \ln \left(\frac{r_k + r_{k+1} - d_k}{r_k + r_{k+1} + d_k} \right)
 \end{aligned} \tag{3.27}$$

$$\begin{aligned}
 \phi_z &= \frac{\partial \phi}{\partial z} \\
 &= \frac{-1}{4\pi} \sum_{k=1}^4 \left[\tan^{-1} \left(\frac{m_k e_k - h_k}{z r_k} \right) - \tan^{-1} \left(\frac{m_k e_{k+1} - h_{k+1}}{z r_{k+1}} \right) \right]
 \end{aligned} \tag{3.28}$$

With,

$$u = \phi_x \cdot \sigma \tag{3.29}$$

$$v = \phi_y \cdot \sigma \tag{3.30}$$

$$w = \phi_z \cdot \sigma \tag{3.31}$$

Second order derivatives of source potential

$$\begin{aligned}
 \phi_{xx} &= \frac{\partial^2 \phi}{\partial x^2} \\
 &= \frac{-1}{4\pi} \sum_{k=1}^4 \frac{2(y_{k+1} - y_k)}{\left((r_k + r_{k+1})^2 - d_k^2\right)} \left(\frac{(x - x_k)}{r_k} + \frac{(x - x_{k+1})}{r_{k+1}} \right) \quad (3.32)
 \end{aligned}$$

$$\begin{aligned}
 \phi_{yx} &= \frac{\partial^2 \phi}{\partial y \partial x} \\
 &= \frac{-1}{4\pi} \sum_{k=1}^4 \frac{-2(x_{k+1} - x_k)}{\left((r_k + r_{k+1})^2 - d_k^2\right)} \left(\frac{(x - x_k)}{r_k} + \frac{(x - x_{k+1})}{r_{k+1}} \right) \quad (3.33)
 \end{aligned}$$

$$\begin{aligned}
 \phi_{zx} &= \frac{\partial^2 \phi}{\partial z \partial x} \\
 &= \frac{-1}{4\pi} \sum_{k=1}^4 \frac{z(y_{k+1} - y_k)(r_k + r_{k+1})}{(r_k r_{k+1}) \cdot \varrho_k} \quad (3.34)
 \end{aligned}$$

$$\begin{aligned}
 \phi_{xy} &= \frac{\partial^2 \phi}{\partial x \partial y} \\
 &= \frac{-1}{4\pi} \sum_{k=1}^4 \frac{2(y_{k+1} - y_k)}{\left((r_k + r_{k+1})^2 - d_k^2\right)} \left(\frac{(y - y_k)}{r_k} + \frac{(y - y_{k+1})}{r_{k+1}} \right) \quad (3.35)
 \end{aligned}$$

(3.33) and (3.35) are equal. Values computed confirm this but developing mathematical proof would be interesting.

$$\begin{aligned}
 \phi_{yy} &= \frac{\partial^2 \phi}{\partial y^2} \\
 &= \frac{-1}{4\pi} \sum_{k=1}^4 \frac{-2(x_{k+1} - x_k)}{\left((r_k + r_{k+1})^2 - d_k^2\right)} \left(\frac{(y - y_k)}{r_k} + \frac{(y - y_{k+1})}{r_{k+1}} \right) \quad (3.36)
 \end{aligned}$$

$$\begin{aligned}
 \phi_{zy} &= \frac{\partial^2 \phi}{\partial z \partial y} \\
 &= \frac{-1}{4\pi} \sum_{k=1}^4 \frac{-z(x_{k+1} - x_k)(r_k + r_{k+1})}{(r_k r_{k+1}) \cdot \varrho_k} \quad (3.37)
 \end{aligned}$$

$$\begin{aligned}
\phi_{xz} &= \frac{\partial^2 \phi}{\partial x \partial z} \\
&= \frac{-1}{4\pi} \sum_{k=1}^4 \frac{2(y_{k+1} - y_k)}{\left((r_k + r_{k+1})^2 - d_k^2\right)} \left(\frac{z}{r_k} + \frac{z}{r_{k+1}}\right)
\end{aligned} \tag{3.38}$$

(note that 3.38 is equal to 3.34)

$$\begin{aligned}
\phi_{yz} &= \frac{\partial^2 \phi}{\partial y \partial z} \\
&= \frac{-1}{4\pi} \sum_{k=1}^4 \frac{-2(x_{k+1} - x_k)}{\left((r_k + r_{k+1})^2 - d_k^2\right)} \left(\frac{z}{r_k} + \frac{z}{r_{k+1}}\right)
\end{aligned} \tag{3.39}$$

(Note that 3.39 is equal to 3.37)

$$\begin{aligned}
\phi_{zz} &= \frac{\partial^2 \phi}{\partial z^2} \\
&= \frac{-1}{4\pi} \sum_{k=1}^4 \frac{\lambda_k \cdot (r_k + r_{k+1})}{(r_k r_{k+1}) \cdot \varrho_k}
\end{aligned} \tag{3.40}$$

Velocity potential for dipole distribution

The velocity potential induced by a dipole distribution of constant unit strength is equivalent to the vertical velocity induced by a constant distribution of sources. Generalizing this statement, we can say that the potential induced by a point dipole oriented in the positive z -axis direction, with unit strength, is equivalent to the z -component of the velocity induced by a unit strength point source.

$$\begin{aligned}
\psi &= \frac{\partial \phi}{\partial z} \\
&= \frac{-1}{4\pi} \sum_{k=1}^4 \left[\tan^{-1} \left(\frac{m_k e_k - h_k}{z r_k} \right) - \tan^{-1} \left(\frac{m_k e_{k+1} - h_{k+1}}{z r_{k+1}} \right) \right]
\end{aligned} \tag{3.41}$$

Velocities induced by dipole distribution

We will take advantage of the relation explained before, stating that the potential induced by a dipole distribution (pointing in the z -direction) is equivalent to the z -component of the velocity induced by a source distribution. Thus, the velocities induced by a dipole distribution will be equivalent to the derivatives of the z -component of the source induced velocity.

Second order derivatives of dipole potential

$$\begin{aligned}
\psi_{xx} &= \frac{\partial^2 \psi}{\partial x^2} \\
&= \frac{-1}{4\pi} \sum_{k=1}^4 \left\{ \frac{z(y_{k+1}-y_k)(r_k+r_{k+1}) \left[-2x + x_k + x_{k+1} - \frac{(x-x_{k+1})r_k}{r_{k+1}} - \frac{(x-x_k)r_{k+1}}{r_k} \right]}{[(r_k r_{k+1}) \cdot \varrho_k^2]} \right. \\
&\quad + \frac{z(y_{k+1}-y_k) \left(\frac{x-x_k}{r_k} + \frac{x-x_{k+1}}{r_{k+1}} \right)}{[(r_k r_{k+1}) \cdot \varrho_k]} - \frac{z(x-x_{k+1})(y_{k+1}-y_k)(r_k+r_{k+1})}{[(r_k r_{k+1}^3) \cdot \varrho_k]} \\
&\quad \left. - \frac{z(x-x_k)(y_{k+1}-y_k)(r_k+r_{k+1})}{[(r_k^3 r_{k+1}) \cdot \varrho_k]} \right\}
\end{aligned} \tag{3.42}$$

$$\begin{aligned}
\psi_{xy} &= \frac{\partial^2 \psi}{\partial x \partial y} \\
&= \frac{-1}{4\pi} \sum_{k=1}^4 \left\{ \frac{z(y_{k+1}-y_k)(r_k+r_{k+1}) \left[-2y + y_k + y_{k+1} - \frac{(y-y_{k+1})r_k}{r_{k+1}} - \frac{(y-y_k)r_{k+1}}{r_k} \right]}{[(r_k r_{k+1}) \cdot \varrho_k^2]} \right. \\
&\quad + \frac{z(y_{k+1}-y_k) \left(\frac{y-y_k}{r_k} + \frac{y-y_{k+1}}{r_{k+1}} \right)}{[(r_k r_{k+1}) \cdot \varrho_k]} - \frac{z(y-y_{k+1})(y_{k+1}-y_k)(r_k+r_{k+1})}{[(r_k r_{k+1}^3) \cdot \varrho_k]} \\
&\quad \left. - \frac{z(y-y_k)(y_{k+1}-y_k)(r_k+r_{k+1})}{[(r_k^3 r_{k+1}) \cdot \varrho_k]} \right\}
\end{aligned} \tag{3.43}$$

$$\begin{aligned}
\psi_{xz} &= \frac{\partial^2 \psi}{\partial x \partial z} \\
&= \frac{-1}{4\pi} \sum_{k=1}^4 \left\{ \frac{z(y_{k+1}-y_k)(r_k+r_{k+1}) \left[-2z - \frac{z r_k}{r_{k+1}} - \frac{z r_{k+1}}{r_k} \right]}{[(r_k r_{k+1}) \cdot \varrho_k^2]} \right. \\
&\quad + \frac{z(y_{k+1}-y_k) \left(\frac{z}{r_k} + \frac{z}{r_{k+1}} \right)}{[(r_k r_{k+1}) \cdot \varrho_k]} - \frac{z^2(y_{k+1}-y_k)(r_k+r_{k+1})}{[(r_k r_{k+1}^3) \cdot \varrho_k]} \\
&\quad \left. - \frac{z^2(y_{k+1}-y_k)(r_k+r_{k+1})}{[(r_k^3 r_{k+1}) \cdot \varrho_k]} + \frac{(y_{k+1}-y_k)(r_k+r_{k+1})}{[(r_k r_{k+1}) \cdot \varrho_k]} \right\} \tag{3.44}
\end{aligned}$$

$$\begin{aligned}
\psi_{yx} &= \frac{\partial^2 \psi}{\partial y \partial x} \\
&= \frac{-1}{4\pi} \sum_{k=1}^4 \left\{ \frac{z(x_{k+1}-x_k)(r_k+r_{k+1}) \left[2x - x_k - x_{k+1} + \frac{(x-x_{k+1})r_k}{r_{k+1}} + \frac{(x-x_k)r_{k+1}}{r_k} \right]}{[(r_k r_{k+1}) \cdot \varrho_k^2]} \right. \\
&\quad - \frac{z(x_{k+1}-x_k) \left(\frac{x-x_k}{r_k} + \frac{x-x_{k+1}}{r_{k+1}} \right)}{[(r_k r_{k+1}) \cdot \varrho_k]} \\
&\quad + \frac{z(x-x_{k+1})(x_{k+1}-x_k)(r_k+r_{k+1})}{[(r_k r_{k+1}^3) \cdot \varrho_k]} \\
&\quad \left. + \frac{z(x-x_k)(x_{k+1}-x_k)(r_k+r_{k+1})}{[(r_k^3 r_{k+1}) \cdot \varrho_k]} \right\} \tag{3.45}
\end{aligned}$$

$$\begin{aligned}
\psi_{yy} &= \frac{\partial^2 \psi}{\partial y^2} \\
&= \frac{-1}{4\pi} \sum_{k=1}^4 \left\{ \frac{z(x_{k+1}-x_k)(r_k+r_{k+1}) \left[2y - y_k - y_{k+1} + \frac{(y-y_{k+1})r_k}{r_{k+1}} + \frac{(y-y_k)r_{k+1}}{r_k} \right]}{[(r_k r_{k+1}) \cdot \varrho_k^2]} \right. \\
&\quad - \frac{z(x_{k+1}-x_k) \left(\frac{y-y_k}{r_k} + \frac{y-y_{k+1}}{r_{k+1}} \right)}{[(r_k r_{k+1}) \cdot \varrho_k]} \\
&\quad + \frac{z(y-y_{k+1})(x_{k+1}-x_k)(r_k+r_{k+1})}{[(r_k r_{k+1}^3) \cdot \varrho_k]} \\
&\quad \left. + \frac{z(y-y_k)(x_{k+1}-x_k)(r_k+r_{k+1})}{[(r_k^3 r_{k+1}) \cdot \varrho_k]} \right\} \tag{3.46}
\end{aligned}$$

$$\begin{aligned}
\psi_{yz} &= \frac{\partial^2 \psi}{\partial y \partial z} \\
&= \frac{-1}{4\pi} \sum_{k=1}^4 \left\{ \frac{z(x_{k+1}-x_k)(r_k+r_{k+1}) \left[2z + \frac{z r_k}{r_{k+1}} + \frac{z r_{k+1}}{r_k} \right]}{[(r_k r_{k+1}) \cdot \varrho_k^2]} \right. \\
&\quad - \frac{z(x_{k+1}-x_k) \left(\frac{z}{r_k} + \frac{z}{r_{k+1}} \right)}{[(r_k r_{k+1}) \cdot \varrho_k]} + \frac{z^2(x_{k+1}-x_k)(r_k+r_{k+1})}{[(r_k r_{k+1}^3) \cdot \varrho_k]} \\
&\quad \left. + \frac{z^2(x_{k+1}-x_k)(r_k+r_{k+1})}{[(r_k^3 r_{k+1}) \cdot \varrho_k]} - \frac{(x_{k+1}-x_k)(r_k+r_{k+1})}{[(r_k r_{k+1}) \cdot \varrho_k]} \right\} \tag{3.47}
\end{aligned}$$

$$\begin{aligned}
\psi_{zx} &= \frac{\partial^2 \psi}{\partial z \partial x} \\
&= \frac{-1}{4\pi} \sum_{k=1}^4 \left\{ \lambda_k \cdot (r_k + r_{k+1}) \cdot \frac{\left[-2x + x_k + x_{k+1} - \frac{(x-x_{k+1})r_k}{r_{k+1}} - \frac{(x-x_k)r_{k+1}}{r_k} \right]}{\left[(r_k r_{k+1}) \cdot \varrho_k^2 \right]} \right. \\
&\quad + \frac{\lambda_k \cdot \left(\frac{x-x_k}{r_k} + \frac{x-x_{k+1}}{r_{k+1}} \right)}{\left[(r_k r_{k+1}) \cdot \varrho_k \right]} - \frac{(x-x_{k+1}) \cdot \lambda_k \cdot (r_k + r_{k+1})}{\left[(r_k r_{k+1}^3) \cdot \varrho_k \right]} \\
&\quad \left. - \frac{(x-x_k) \cdot \lambda_k \cdot (r_k + r_{k+1})}{\left[(r_k^3 r_{k+1}) \cdot \varrho_k \right]} - \frac{(y_{k+1}-y_k)(r_k + r_{k+1})}{\left[(r_k r_{k+1}) \cdot \varrho_k \right]} \right\}
\end{aligned} \tag{3.48}$$

$$\begin{aligned}
\psi_{zy} &= \frac{\partial^2 \psi}{\partial z \partial y} \\
&= \frac{-1}{4\pi} \sum_{k=1}^4 \left\{ \lambda_k \cdot (r_k + r_{k+1}) \cdot \frac{\left[-2y + y_k + y_{k+1} - \frac{(y-y_{k+1})r_k}{r_{k+1}} - \frac{(y-y_k)r_{k+1}}{r_k} \right]}{\left[(r_k r_{k+1}) \cdot \varrho_k^2 \right]} \right. \\
&\quad + \frac{\lambda_k \cdot \left(\frac{y-y_k}{r_k} + \frac{y-y_{k+1}}{r_{k+1}} \right)}{\left[(r_k r_{k+1}) \cdot \varrho_k \right]} - \frac{(y-y_{k+1}) \cdot \lambda_k \cdot (r_k + r_{k+1})}{\left[(r_k r_{k+1}^3) \cdot \varrho_k \right]} \\
&\quad \left. - \frac{(y-y_k) \cdot \lambda_k \cdot (r_k + r_{k+1})}{\left[(r_k^3 r_{k+1}) \cdot \varrho_k \right]} - \frac{(x_{k+1}-x_k)(r_k + r_{k+1})}{\left[(r_k r_{k+1}) \cdot \varrho_k \right]} \right\}
\end{aligned} \tag{3.49}$$

$$\begin{aligned}
\psi_{zz} &= \frac{\partial^2 \psi}{\partial z^2} \\
&= \frac{-1}{4\pi} \sum_{k=1}^4 \left\{ \lambda_k \cdot (r_k + r_{k+1}) \cdot \frac{\left[-2z - \frac{z r_k}{r_{k+1}} - \frac{z r_{k+1}}{r_k} \right]}{\left[(r_k r_{k+1}) \cdot \varrho_k^2 \right]} + \frac{\lambda_k \cdot \left(\frac{z}{r_k} + \frac{z}{r_{k+1}} \right)}{\left[(r_k r_{k+1}) \cdot \varrho_k \right]} \right. \\
&\quad \left. - \frac{z \cdot \lambda_k \cdot (r_k + r_{k+1})}{\left[(r_k r_{k+1}^3) \cdot \varrho_k \right]} - \frac{z \cdot \lambda_k \cdot (r_k + r_{k+1})}{\left[(r_k^3 r_{k+1}) \cdot \varrho_k \right]} \right\}
\end{aligned} \tag{3.50}$$

3.4 Solving the Discretized Integral Equation

The discretized integral equation 3.10 can be written as a system of linear equations as follows

$$\begin{bmatrix} a_{11} & a_{12} \dots & a_{1,N_b} \\ a_{21} & a_{22} \dots & a_{2,N_b} \\ \vdots & \vdots & \vdots \\ a_{N_b,1} & a_{N_b,1} \dots & a_{N_b,N_b} \\ \vdots & \vdots & \vdots \\ a_{N_b+N_f,1} & a_{N_b+N_f,1} \dots & a_{N_b+N_f,N_b} \end{bmatrix} \begin{bmatrix} \sigma_1 \\ \sigma_2 \\ \vdots \\ \sigma_{N_b} \end{bmatrix} + \quad (3.51)$$

$$\begin{bmatrix} b_{1,1} \dots b_{1,N_b} & c_{1,N_b+1} \dots c_{1,N_b+N_w} \\ b_{2,1} \dots b_{2,N_b} & c_{2,N_b+1} \dots c_{2,N_b+N_w} \\ \vdots & \vdots \\ b_{N_b,1} \dots b_{N_b,N_b} & c_{N_b,N_b+1} \dots c_{N_b,N_b+N_w} \\ \vdots & \vdots \\ b_{N_b+N_f,1} \dots b_{N_b+N_f,N_b} & c_{N_b+N_f,N_b+1} \dots c_{N_b+N_f,N_b+N_w} \end{bmatrix} \begin{bmatrix} \mu_1 \\ \mu_2 \\ \vdots \\ \mu_{N_b} \\ \mu_{N_b+1} \\ \vdots \\ \mu_{N_b+N_w} \end{bmatrix} + \quad (3.52)$$

$$\begin{bmatrix} a_{1,N_b+N_w+1} \dots & a_{1,N_b+N_w+N_f} \\ a_{2,N_b+N_w+1} \dots & a_{2,N_b+N_w+N_f} \\ \vdots & \vdots \\ a_{N_b,N_b+N_w+1} \dots & a_{N_b,N_b+N_w+N_f} \\ \vdots & \vdots \\ a_{N_b+N_f,N_b+N_w+1} \dots & a_{N_b+N_f,N_b+N_w+N_f} \end{bmatrix} \begin{bmatrix} \sigma_{N_b+1} \\ \sigma_{N_b+2} \\ \vdots \\ \sigma_{N_b+N_f} \end{bmatrix} = \quad (3.53)$$

$$\begin{bmatrix} U_b^T \cdot \underline{n}_1 \\ U_b^T \cdot \underline{n}_2 \\ \vdots \\ U_b^T \cdot \underline{n}_{N_b} \\ 0 \\ 0 \\ 0_{n_b+N_f} \end{bmatrix} \quad (3.54)$$

The above system of equations can be manipulated as follows. We will assume for each panel, that the source strength σ is equal to the normal component of the velocity at infinity for that panel $\underline{n}^T \cdot \underline{U}_b$. As a result, we can move the source strength matrix to the write hand side of the equation.

At this point our unknowns are the source strength for each free surface panel, and the dipole strength for the body panels and the wake panels. Never the less, in order to satisfy the Kutta condition, we will require that for each chord-wise strip of panels, the dipole strength on the first wake panel will be equal to the difference between the dipole strength of the upper foil surface trailing edge panel and the dipole strength of the lower foil surface trailing edge panel. All the wake panels will have the same dipole strength on each chord-wise strip of panels. This implementation of the Kutta condition is based on the lumped-vortex element approach, used to solve 2-D lifting problems (Katz & Plotkin, 2001, see Chapter 5 p. 114). For details on the implementation of the Kutta condition see Katz & Plotkin (2001).

A consequence of the above statement is that we do not have additional unknowns for the dipole strength of the wake panels. They can be expressed in terms of the dipole strength of the foil upper surface and lower surface trailing edge panels, for each strip of panels in the chord-wise direction.

All the above facts will allow us to solve the system of linear equations, which will have a total of $N_b + N_f$ unknowns. The unknowns will be the dipole strength of the body panels N_b , and the source strength for the free surface panels N_f .

For details about the method of solution described above see Chapter 12 in Katz & Plotkin (2001).

There are different methods of solution to solve the source and the doublet strength. For the most part, all method will make an assumption about the source strength or the dipole strength, and then solve for only one singularity. This is possible since there are infinite possible combinations of dipole strengths and source strengths, and everyone of this combinations will yield a unique solution to the problem. Recall that the unique solution will satisfy the Laplace equation and the boundary conditions. For additional methods of solution for the dipole and source strength on the lifting flow problem see Katz & Plotkin (2001) and Hess (1972). We will now describe briefly the method of solution by Hess (1972).

3.4.1 The Method by Hess and Smith

The lifting problem we are dealing with was initially solved by Hess (1972). On this method, dipoles and sources are used to solve the problem. They distribute sources and dipoles on the foil surface, and use only dipoles for the wake panels.

This method uses panels with a constant source strength distributed over each foil panel. For the dipole strengths, it is used a linearly varying dipole strength distributed over the panel.

The foil surface is discretized, so that the panels are numbered and grouped in longitudinal lifting strips. Each lifting strip starts at the trailing edge on the foil lower surface, numbering the panels sequentially towards the leading edge. The lifting strip then continues on the upper foil surface, numbering the panels sequentially towards the trailing edge. The lifting strip is

then extended longitudinally aft of the trailing edge with the wake panels.

At each lifting strip the dipole strength is fixed to zero at the trailing edge on the foil lower surface. The dipole strength would linearly vary with the distance of each panel to the trailing edge. This distance is measured as an arc length, starting at the trailing edge and continuing to the leading edge on the lower foil surface, and all the way around the foil contour on the upper foil surface back to the trailing edge.

The dipole strength of the wake panels on each strip would be equal to the dipole strength of the upper surface trailing edge panel. This, because the panel at the lower surface trailing edge has zero dipole strength, and the dipole strength on the wake panels is equal to the difference between the dipole strength of the upper trailing edge panel and the lower trailing edge panel.

Hess and Smith apply an additional condition that requires the flow to leave the foil along the bisector of the trailing edge. This condition is also called tangency condition. This flow condition is applied at Kutta points located a small distance aft of the trailing edge. The flow tangency approach gives additional equations for the dipole strengths that are of the same type as in the case of body source panels. There will be as many Kutta points as lifting strips (one kutta point per lifting strip).

Setting up the problem as described above, allows us to obtain an equation for the dipole strength on each panel of a lifting strip. Basically, the dipole strength on each panel on a lifting strip will be equal to the product of its distance to the trailing edge (arc length), times a proportionality constant for each lifting strip. The unknown in the system of linear equations will be the proportionality constant for each lifting strip.

The influence of each lifting strip on all the collocation points, will be collected by summing up the influence of each of the panels of the lifting strip. Thus, as explained above, we will add one column and one row per each lifting strip to the system of linear equations that results for the source strength. The additional rows on the equations will capture the effect on the Kutta points, the additional columns will retrieve the effect of the lifting strips.

For a detailed description of the method by Hess and Smith see Hess (1972) and Janson (1997).

Chapter 4

Results and Conclusions

4.1 Deeply submerged Foil

For the deeply submerged implementation we used the foil profile NACA2415. This foil profile has a mid-line with 2% maximum camber. The maximum camber will be at 0.4 of the chord length, measured from the leading edge. We tested the foil at a 6 degrees angle of attack, and a Froude number of 0.7. The foil has an aspect ration of 4. We discretized the foil with 20 panels in the chord-wise direction, and 40 panels span-wise for the half foil span we modeled. The negative half span of the model was accounted for using a mirror image. We discretized the wake identically to the foil in the transverse direction with 40 panels. In the longitudinal direction we used 120 panels for the wake. For detailed description of classical foil profiles see Abbott and Doenhoff Abbott & Von Doenhoff (1959). See figure 4.1 for the discretized foil geometry.

For the current implementation we used the method described by Katz and Plotkin, see Katz & Plotkin (2001). For a short description of the method see 3.4.

The results for the pressure coefficient obtained for the deeply submerged foil case described above, can be observed in figure 4.2. In figure 4.3, we can observed a view of the same foil looked from below. It can be seen on the figures that the pressure coefficient at the trailing edge is the same for the upper and lower surface, which verifies that the tangency flow condition has been enforced correctly (Kutta condition). We can also observe the difference in the pressure coefficient between the upper and lower surface. The smaller pressure coefficient in the upper foil surface compared to the higher pressure coefficient in the lower surface, implies that there will be a resultant pressure vertically up. Note that the shown result includes the effect of the wake panels. A little less noticeable, it can be observed a reduction in the difference of the pressure coefficient between the upper and lower surface of the foil, as we approach the foil side

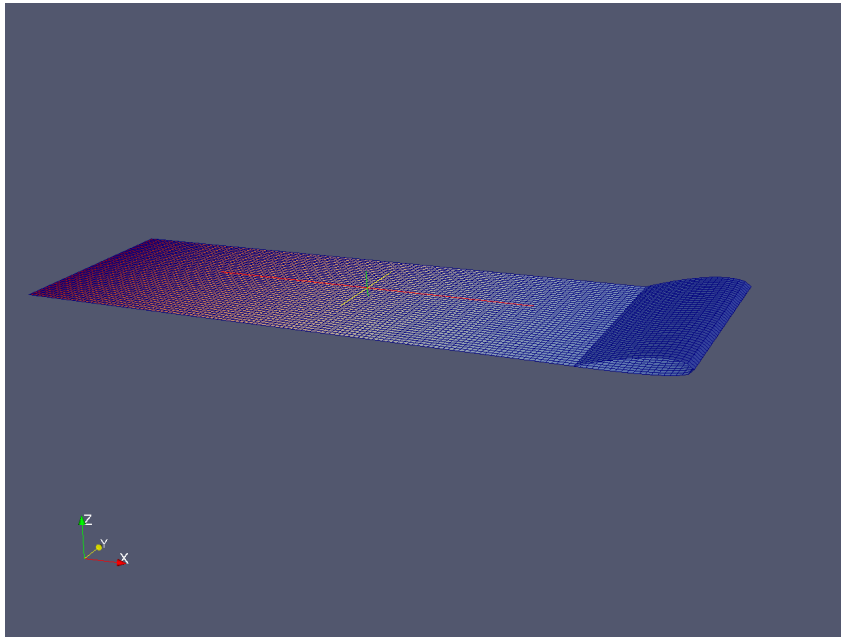


Figure 4.1: Foil geometry discretization NACA2415

end.

The figure 4.4, shows a result comparison between the lifting program ‘HL’ develop as part of this thesis work and the program Xfoil by Selig (1996). The program Xfoil is a research effort development validated experimentally. Details can be found in the cited reference. On figure 4.5 we can observe a table comparing the results between our code HL and the program XFOIL. By looking at the figures we can observe that the biggest difference in the results between the two programs is in the velocity distribution on the foil upper surface. Basically, our program HL is over predicting the velocity on the foil upper surface. It should be noted that an increase in the number of panels used in our implementation HL, should bring its results closer to the XFOIL results. The first hump in the velocity distribution curve on the foil upper surface will tend to move forward as we increase the number of panels on HL, and the velocity drop near the trailing edge will tend to move aft.

Figure 4.6 shows the pressure coefficient c_p , for a deeply submerged foil NACA0012, at a zero angle of attack. Because of the symmetric geometry of the foil, and the zero angle of attack, it can be seen that there is no lift developed on the foil. As it can be observed, the pressure distribution is symmetric, presenting the same values in the upper and lower surface. It is important to mention that to model this case we only used a source distribution, i.e. source panels, in order to model the thickness problem. Figure 4.7 shows a comparison between different discretizations and Froude numbers for the fully submerged foil case with no lift. Note that the lines for the velocity distribution for the lower and upper foil surface will be on top of each other for each discretization case. This, because the velocities are equal in the foil upper and lower

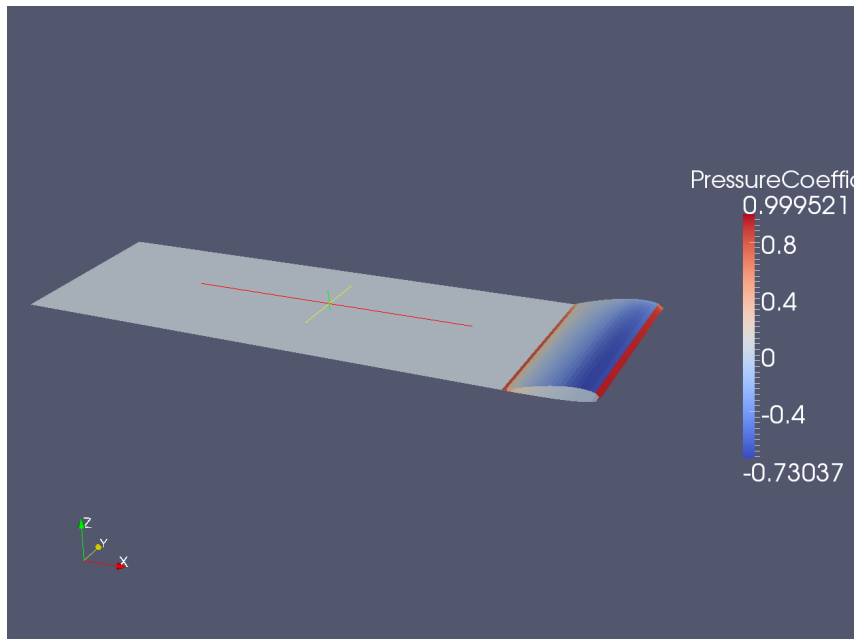


Figure 4.2: Pressure coefficient c_p . NACA2415 deeply submerged, angle of attack 6 deg. Froude number $F_n = 0.7$

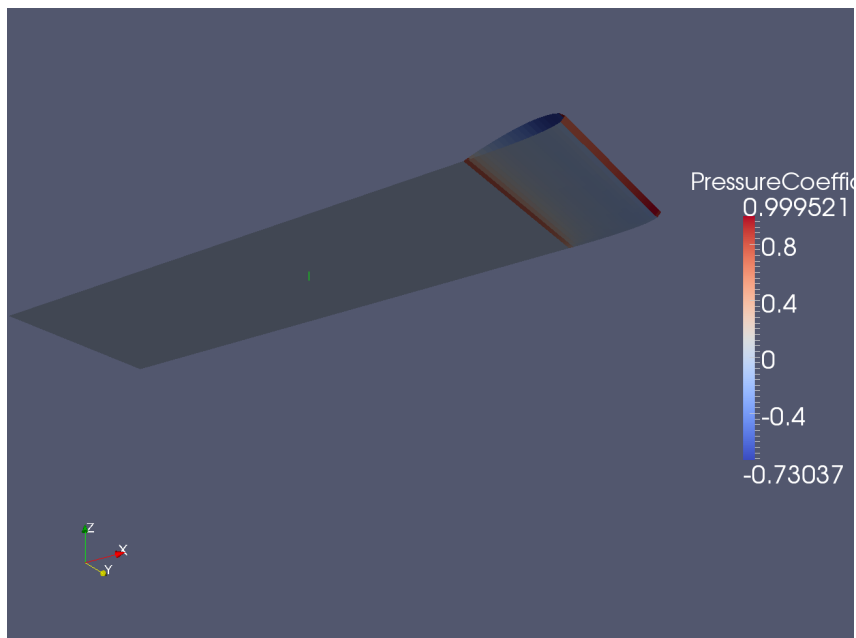


Figure 4.3: Pressure coefficient c_p . NACA2415 deeply submerged, angle of attack 6 deg. Froude number $F_n = 0.7$

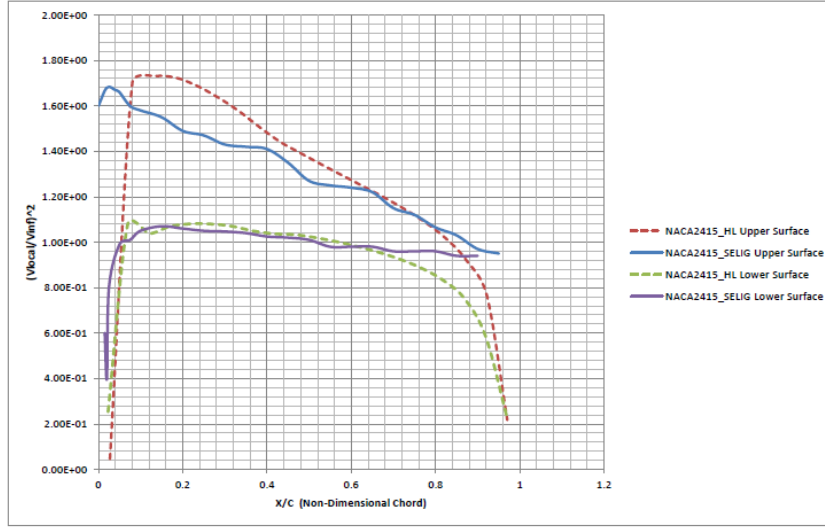


Figure 4.4: Velocity Distribution $(V/V_\infty)^2$. NACA2415 deeply submerged, angle of attack 6 deg. Froude number $Fn = 0.7$. Result comparison between program XFOIL by Selig (validated experimentally), and the lifting program HL produced as part of this thesis

surface. As shown in the figure, as we increase the number of panels, specifically in the chord-wise direction, the velocity distribution curve hump on the upper foil surface tends to appear or move forward. Also, observe that the velocity reduction or velocity drop near the trailing edge tends to appear further aft. Regarding the effect of the Froude number, it can be seen that it has no effect on the velocity distribution, and consequently on the pressure coefficient. On the figure, the green dashed lines correspond to the velocity distribution for a discretization of 20 panels chord-wise and a Froude Number of 0.7, and the blue dotted lines correspond also to a discretization of 20 panels chord-wise, but with a Froude number of 0.3. Note that the two lines are on top of each other, meaning the velocity distribution is the same for both cases.

Figure 4.8, shows the results for the pressure coefficient cp for a fully submerged foil NACA0012, with an angle of attack of 6 degrees. The foil has an aspect ratio of 4, and a discretization with 20 panels in the chord-wise direction, and 40 panels span-wise for the half foil modeled. The negative half span of the foil was modeled using a mirror image technique. From the figure, it can be observed that the pressure coefficient cp is asymmetric, and as a result a lifting force is developed. The smaller pressure coefficient on the foil upper surface, compared to the higher pressure coefficient on the foil lower surface, indicates that a resultant force directed vertically up will be obtained. Additionally, note that the pressure coefficient values obtained in the foil lower and upper surface at the trailing edge are equal. This verifies the presence of a flow tangency condition at the trailing edge, satisfying the Kutta condition.

On figure 4.9, we can observe a comparison for the velocity distribution $[(V/V_\infty)^2]$, between a NACA0012 foil fully submerged, running at a zero angle of attack; and the same foil fully

Comparison for the values of $(V / V_{\infty})^2$ - HL vs. XFOIL (by Selig)			
X - Coordinate	HL- Code	X-Foil	Percent Difference
1.675	4.63E-02	1.675	-97.23772937
1.6	1.7023461	1.6	6.39663125
1.56	1.730367	1.56	10.92096154
1.52	1.7241453	1.52	13.43061184
1.48	1.6886503	1.48	14.09799324
1.45	1.6377844	1.45	12.95064828
1.425	1.5773159	1.425	10.68883509
1.415	1.5059971	1.415	6.430890459
1.38	1.4406361	1.38	4.39392029
1.3	1.3901515	1.3	6.934730769
1.26	1.3405846	1.26	6.395603175
1.245	1.2926596	1.245	3.828080321
1.23	1.2452196	1.23	1.237365854
1.19	1.1967307	1.19	0.565605042
1.13	1.1450823	1.13	1.334716814
1.08	1.0870033	1.08	0.648453704
1.04	1.0165343	1.04	-2.256317308
1	0.92013198	1	-7.986802
0.96	0.76525369	0.96	-20.28607396

Figure 4.5: Result comparison for velocity distribution $(V/V_{\infty})^2$ on foil upper surface, between program XFOIL by Selig (validated experimentally), and the lifting program HL produced as part of this thesis. NACA2415 deeply submerged, angle of attack 6 deg. Froude number $Fn = 0.7$

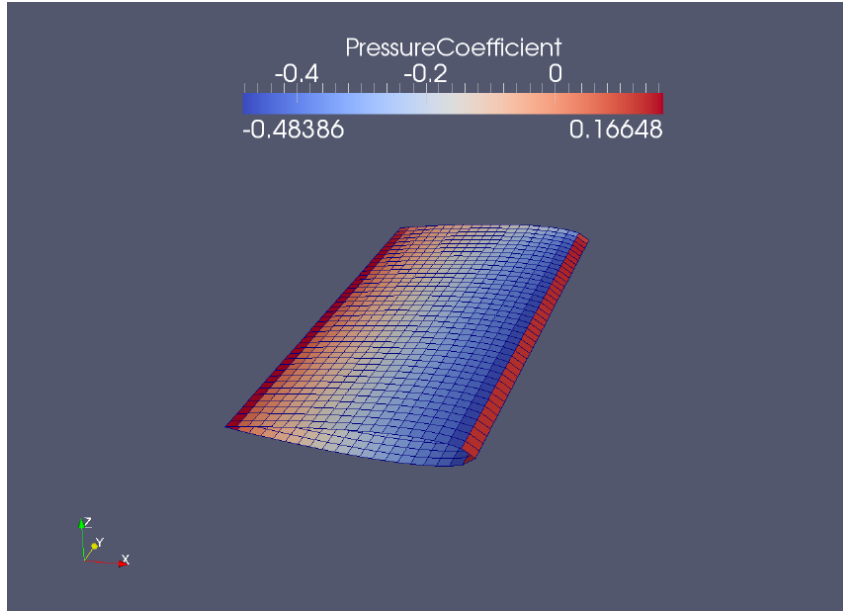


Figure 4.6: Pressure coefficient c_p . NACA0012 deeply submerged, zero angle of attack.

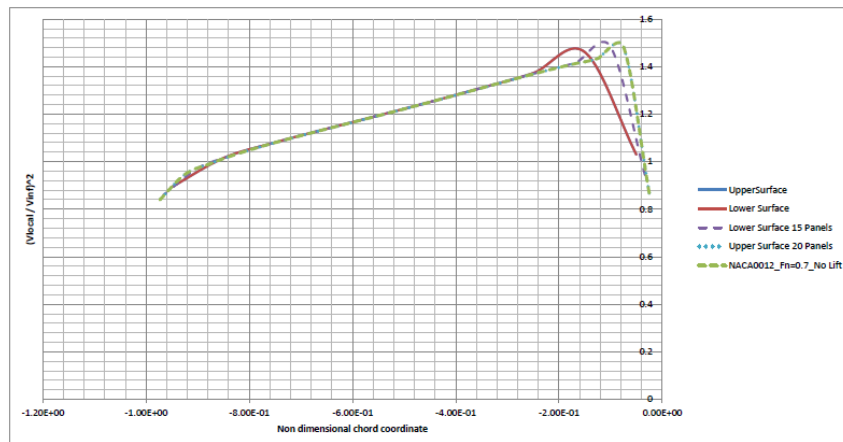


Figure 4.7: Velocity Distribution $(V/V_\infty)^2$. NACA0012 deeply submerged, zero angle of attack. Discretization effect comparison, and Froude number effect

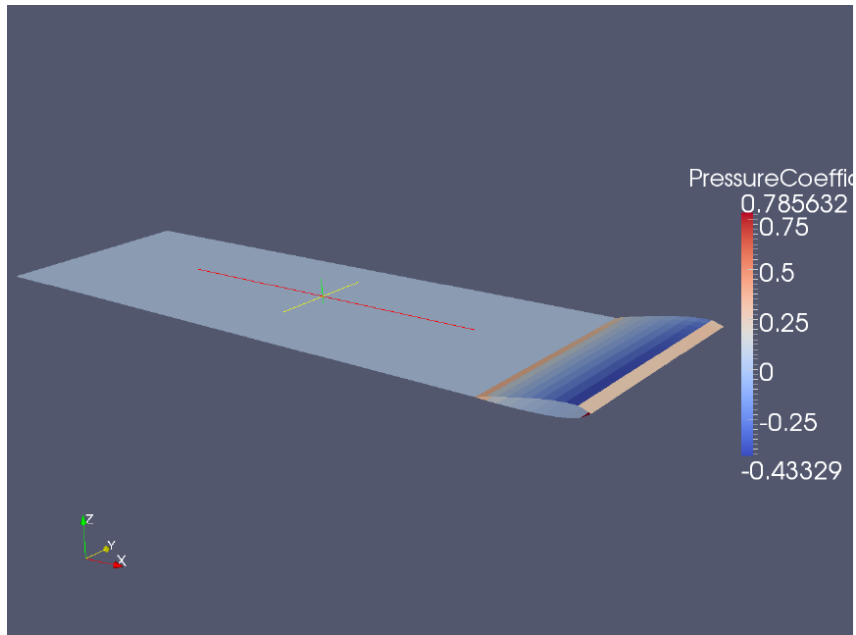


Figure 4.8: Pressure coefficient. NACA0012 deeply submerged. Aspect ratio 4. Angle of attack 6 degrees . 20 foil panels chord-wise. 120 wake panels in the longitudinal direction

submerged, running at a 6 degrees angle of attack. The blue dashed line shows the velocity distribution for the upper and lower surface, for the foil running at a zero angle of attack. The green continuous line shows the velocity distribution of the upper surface, for the foil running at 6 degree angle of attack. The purple continuous line shows the velocity distribution of the lower surface, for the foil running at 6 degree angle of attack. In both cases the same discretization was used. For the lifting case with the foil running at 6 degrees angle of attack, the wake was included in the geometry. We can see on the figure, that the velocity distribution for the zero angle of attack foil, is similar to the one obtained for the foil upper surface with the foil at 6 degrees angle of attack. We can observe that there is a significant difference for the velocity distribution on the lower foil surface, when comparing the lifting and the non-lifting case. We can see a velocity reduction on the lower foil surface when the foil is running at an angle of attack.

In figure 4.10, we can observe the effect of the foil geometry discretization on the foil velocity distribution. The figure compares two different discretizations for the NACA0012 foil running at a 6 degrees angle of attack. For a discretization using 10 panels chord-wise, the blue dashed lines represent the velocity distribution of the foil upper surface, and the red dashed lines represent the velocity distribution on the foil lower surface. For a discretization using 25 panels chord-wise, the light blue lines represent the velocity distribution of the foil upper surface, and the pink lines represent the velocity distribution on the foil lower surface. This plot is basically self explanatory, showing how the results get more accurate as the discretization is refined.

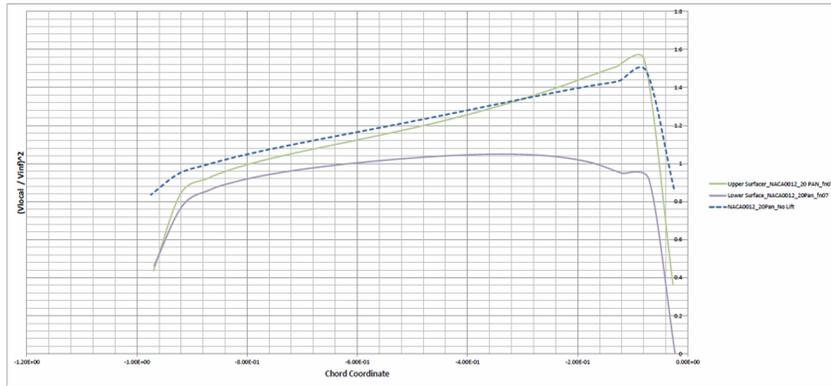


Figure 4.9: Velocity Distribution $(V/V_\infty)^2$. NACA0012 deeply submerged, zero angle of attack no lifting foil vs. lifting case with foil at a 6 degrees angle of attack. Foil discretization 20 panels chord-wise. Froude number $Fn = 0.7$.

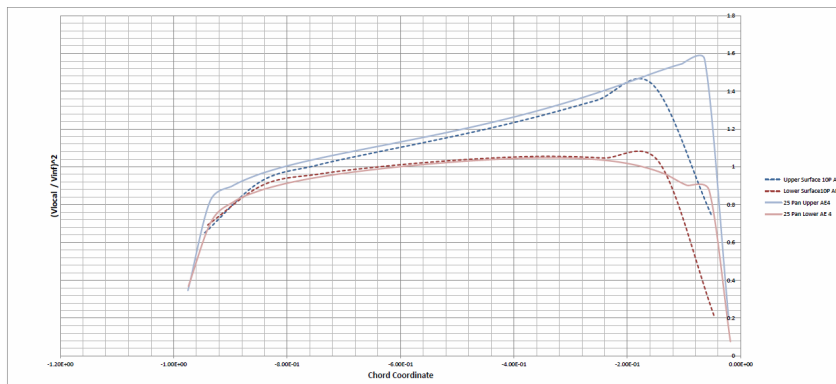


Figure 4.10: Velocity Distribution $(V/V_\infty)^2$. NACA0012 deeply submerged, Foil at 6 Degrees angle of attack. Effect of foil discretization 10 panels chord-wise (dotted lines) vs. 25 panels chord-wise (continuous lines). On both cases the Froude number $Fn = 0.7$, and aspect ration 4

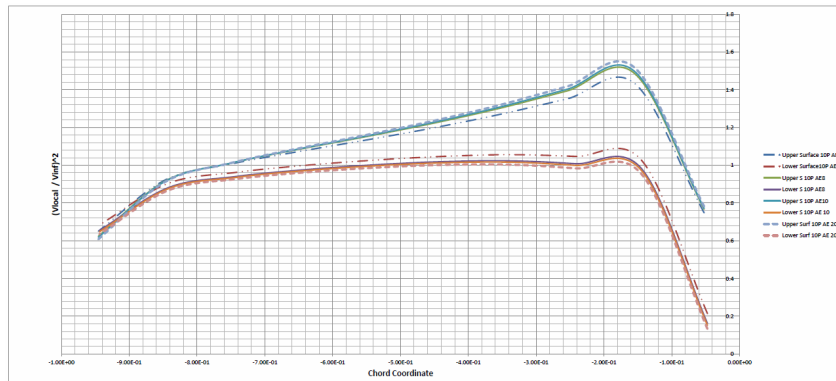


Figure 4.11: Velocity Distribution $(V/V_\infty)^2$. NACA0012 deeply submerged, Foil at 6 Degrees angle of attack. Foil aspect ratio effect on the pressure distribution. Aspect ratio 4 (dot and dash lines) vs. aspect ratio 8 (purple and green continuous lines). vs. aspect ratio 10 (orange and blue continuous lines) vs. aspect ratio 20 (dashed lines). Froude number $Fn = 0.7$

Figure 4.11, shows the effect of the variation of the aspect ratio on the velocity distribution over the foil upper and lower foil surfaces. For this plot we tested a foil NACA0012, at an angle of attack of 6 degrees, and a Froude number of 0.7. The foil was discretized with 10 panels in the chord-wise direction. In all cases the aspect ration of the panels was kept equal to one. The wake was discretized with 120 panels in the longitudinal direction, and as many panels as the foil for the span-wise direction. From the figure, we can observe that the difference in the local velocity between the foil upper and lower surface, increases as we augment the aspect ratio. The higher the aspect ratio, the greater will be the difference between the velocities in the upper and lower surface. This implies that with a higher aspect ratio we will obtain more lift, as expected.

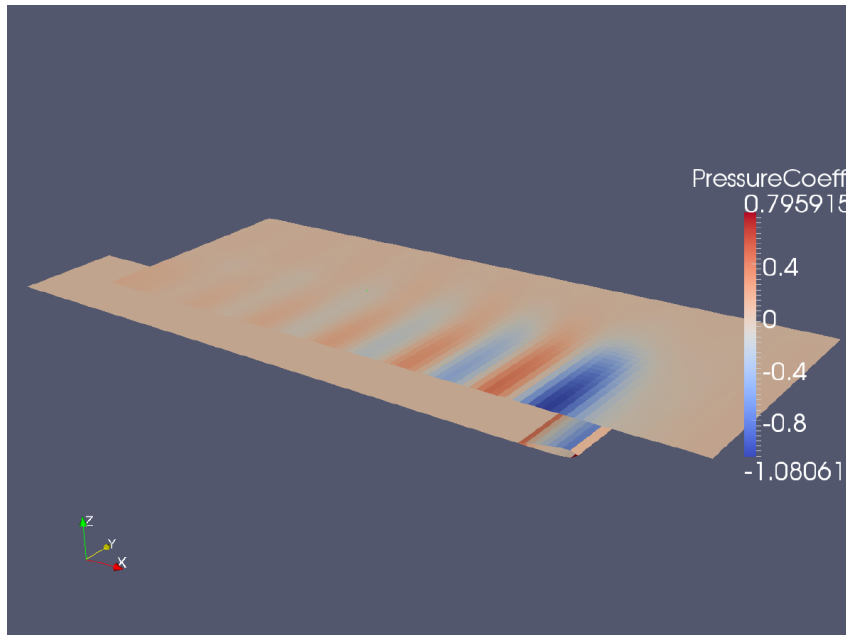


Figure 4.12: Pressure coefficient. NACA0012 Submerged at 0.5 Chord length. Aspect ratio 4. Angle of attack 6 degrees

4.2 Submerged Foil Close to the Free Surface

For the modeling of a foil running close to the free surface we used the NACA0012 profile. In figure 4.12, we can observe the results for the pressure coefficient cp , on the hydrofoil body, as well as on the free surface. The foil is tested at an angle of attack of 6 degrees. The foil aspect ratio is 4. The foil is discretized with 8 panels chord-wise on the body surface. The wake has 80 panels in the longitudinal direction and, as many panels as the foil on the span-wise direction. The free surface has 80 panels in the longitudinal direction, and 2 times as many panels as the foil in the transverse direction. Note that with the current discretization, the wake will be extending further aft than the free surface a total of three chord lengths. Looking at the results, we can observe a negative pressure coefficient on the free surface above the foil. This is caused by the higher velocity on the upper foil surface, which affect the free surface accelerating the water particles, and consequently creating the wave trough. See also figure 4.14 for the wave elevation to observe this characteristic of the free surface. We can also observe, that the free surface presents a wave crest which is aligned or located longitudinally aft of the trailing edge. This correlates with the velocity reduction on the flow over the foil upper surface as the trailing edge is approached. Additionally, note that the pressure coefficient cp at the trailing edge, has the same value on the upper and lower foil surfaces. This verifies that the Kutta condition requiring the flow to leave the trailing edge in a tangent fashion is enforced correctly.

Figure 4.15 shows the wave profile for the foil case shown on figure 4.13 and figure 4.12. Note

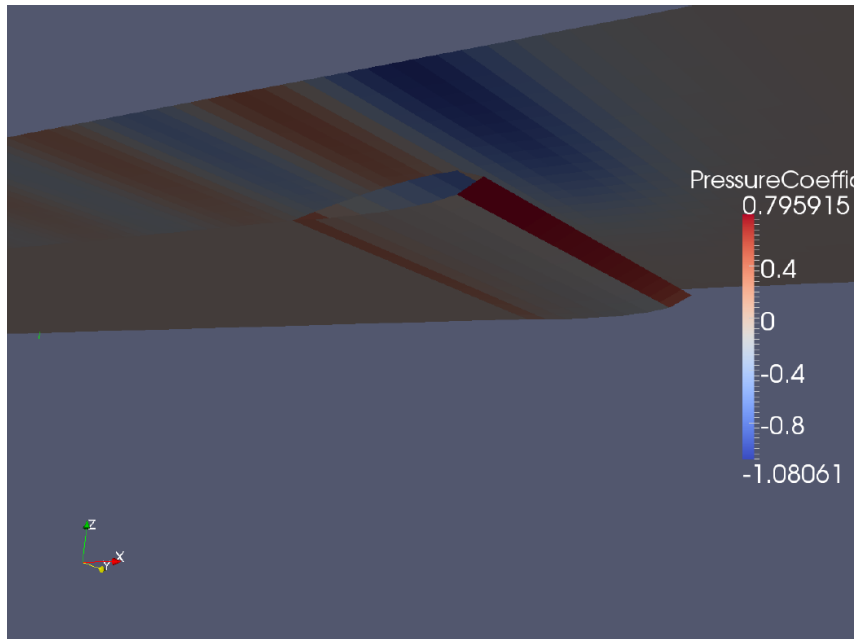


Figure 4.13: Pressure coefficient. NACA0012 Submerged at 0.5 Chord length. Aspect ratio 4. Angle of attack 6 degrees

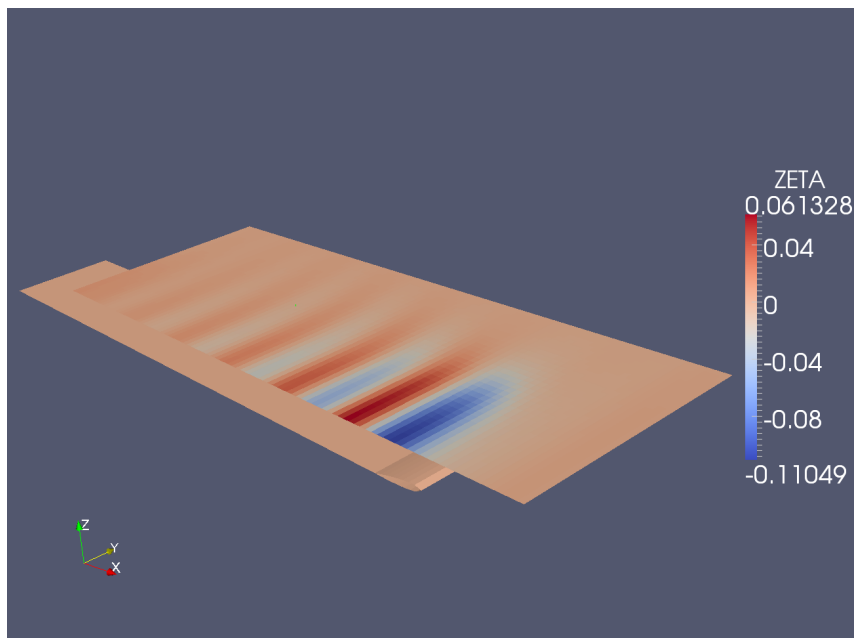


Figure 4.14: Wave Elevation. NACA0012 submerged at 0.5 Chord length. Aspect ratio 4. Angle of attack 6 degrees. Froude number 0.5

that the plot is not to scale. This wave profile is computed in the strip of free surface panels above the foil center line. The chord length of our foil is one, thus, a wave height of 0.06 would imply a wave height of 6 % of the chord length. All the plotted cases are for the foil submerged 0.5 chord lengths, a Froude number of 0.5, and a foil aspect ratio of 4. On the computational implementation, the collocation points on the free surface are shifted forward in order to account for the radiation condition. Basically, if we obtain waves radiated forward of the foil, that would not be mathematically incorrect. Thus, the forward shift in the collocation points on the free surface is used to make sure that the waves will appear aft of the foil. We observed in our implementation, that the wave height was affected by the forward shift on the free surface collocation points. We also observed that the wave height was affected by the extension of the free surface, and the wake, aft of the foil trailing edge. The blue line shows a run of the program with the free surface, and the wake, extending eight chord lengths aft of the trailing edge. We can observe that there is a rise on the level of the free surface towards its aft end. This is coincident with the Helmholtz theorem which states that vorticity cannot end, nor start in the flow. Thus, we would have to extend the wake aft to infinity, since the wake contains the trailing vorticity generated on the foil. Note that on the wake, the last span-wise segment of vortices, corresponding to the last span-wise strip of panels, is not cancelled out. Hence, this span-wise vortex segment will affect the free surface, producing a velocity reduction, and consequently, a rise in the free surface level towards the aft end of the free surface.

On the figure 4.15, the mustard-yellow coloured line represents a run of the foil, with the free surface extending 7 chord lengths aft of the trailing edge, and the wake extending 12 chord lengths aft of the trailing edge. Additionally, we used a forward shift on the Free surface collocation points of 0.85 panel lengths. In all other cases we used a forward shift in the free surface collocation points of 0.72 panel lengths. It can be seen that for this case we obtained the highest wave amplitude. Note that, for the light blue line we used the same geometry configuration in terms of the wake and free surface lengths; but with a forward shift on the free surface collocation points of 0.72 panel lengths; and the obtained wave amplitude is smaller. We noted that by increasing the shift in the free surface collocation points, we will get an increase on the wave amplitude.

The light pink line on the figure 4.15, shows a run of the foil with the free surface extending seven chord lengths aft of the foil trailing edge, and the wake extending twelve chord lengths aft of the trailing edge. Note that the wave amplitude is the same as for all the other cases with a forward shift on the free surface collocation points of 0.72 chord lengths. Finally, the green line of the figure, shows a run of the foil with the free surface extending nine chord lengths aft of the trailing edge, and the wake extending twelve chord lengths aft of the trailing edge. We can still observe the free surface rising towards its aft end. We also observe that by extending the free surface aft enough, we obtain a better picture of how the disturbance due to the foil dissipates far aft from it.

Despite the sensitivity shown by the program HL, to the forward shift on the free surface collocation points, as well as the extension of the wake, and the free surface aft of the foil. We can observe a good overall convergence on the results. This, provided good modelling practices

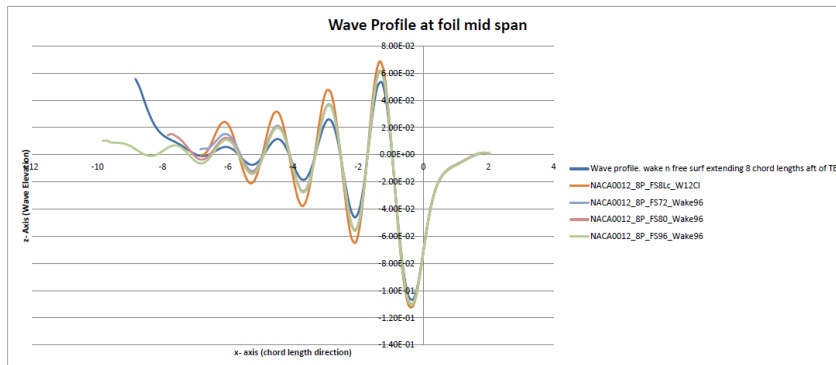


Figure 4.15: Pressure coefficient. NACA0012 submerged at 0.5 Chord length. Aspect ratio 4. Angle of attack 6 degrees. Froude number 0.5

are employed, and the assumptions of the potential flow theory for lifting flows are properly accounted for.

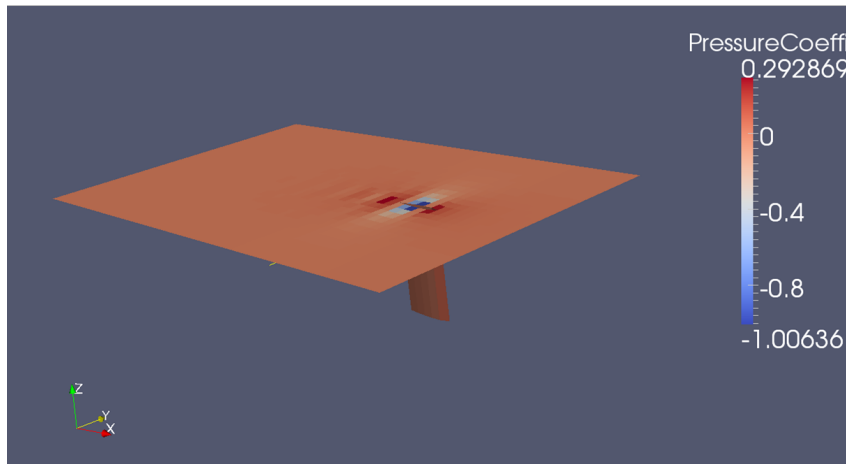


Figure 4.16: Pressure coefficient. NACA0012 Surface piercing foil. Zero angle of attack. No lift. Froude number 0.3.

4.3 The Free Surface Piercing Foil

In figure 4.16 and figure 4.17, we can observe the results obtained when testing the surface piecing foil running at a zero angle of attack, which produces no lift. To test the program we used the foil profile NACA0012. In figure 4.17, we can see the wave field produced for this particular case. As indicated in the plot, we see that the wave trough reaches a depth below the calm free surface level of approximately 4.8% the foil chord length. The wave crest reaches a height above the calm free surface level of approximately 2% the foil chord length. Even though we do not have data for a direct comparison of the wave field; the solution we obtained for the foil at zero angle of attack, is in appearance very similar to the solution obtained by Janson on his Report No. 96:40. See Janson Janson (1997). In comparison with Janson's results, we should point out that around the foil, the wave elevations and the shape of the wave field are very similar to our results; but aft of the foil trailing edge, Janson's results show a wider wave in the transverse direction, and the wave field seems to extend further aft than in the results obtained by our program HL.

In Figure 4.18, we can observe the result for the wave field and the wave elevation for a surface piercing foil NACA0012 running at 6 degrees angle of attack. For this case we found that our program was not producing consistent results. Generally, the program would yield different values for the pressure coefficient cp and the wave elevation z , when the discretization was changed. Never the less, the obtained wave field was consistent in appearance regardless of the difference on the wave heights. This kind of inconstancy, is believed to be caused by some kind of singularity issue.

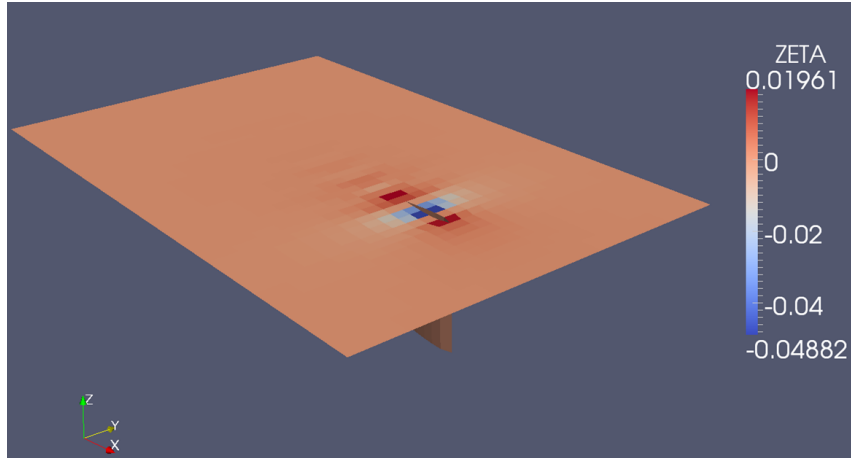


Figure 4.17: Wave elevation. NACA0012 Surface piercing foil. Zero angle of attack. No lift. Froude number 0.3.

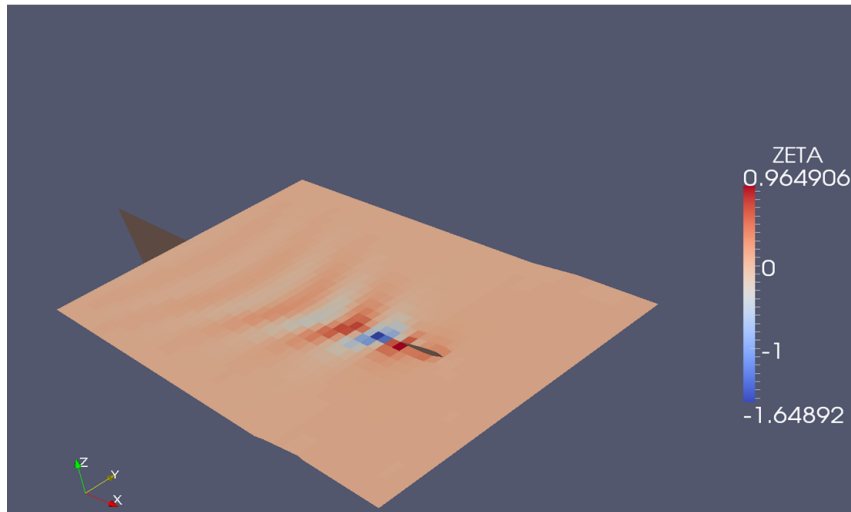


Figure 4.18: Wave elevation. NACA0012 Surface piercing foil. Angle of attack 6 degrees. Froude number 0.3.

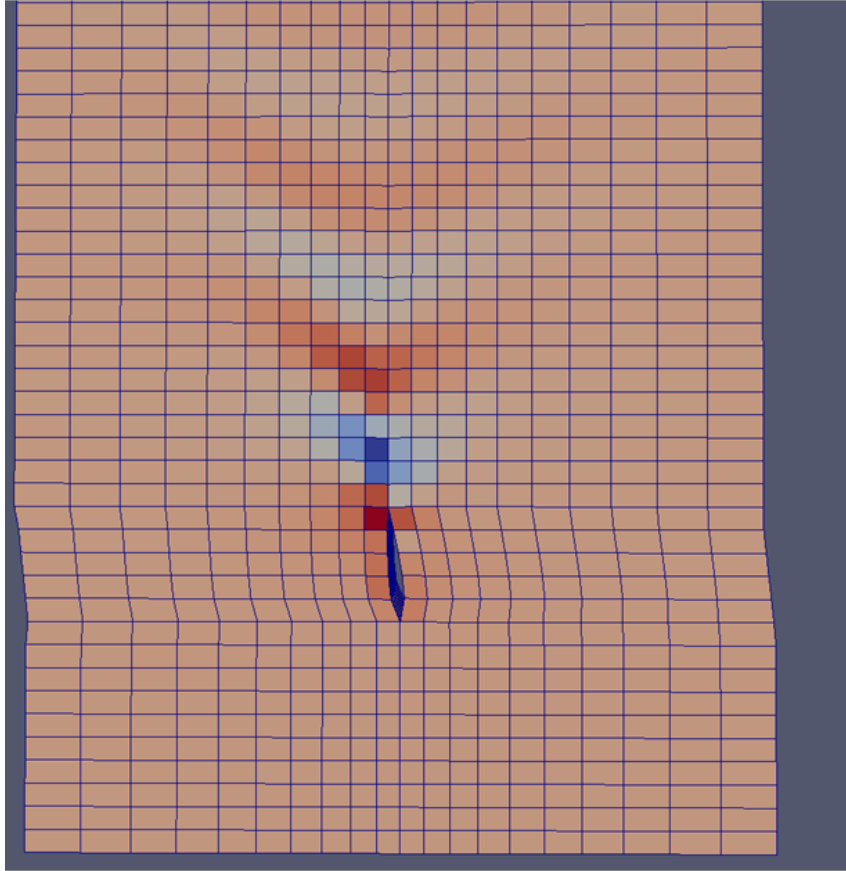


Figure 4.19: Wave elevation. NACA0012 Surface piercing foil. Angle of attack 6 degrees. Froude number 0.3.

Bibliography

- Abbott, I. & Von Doenhoff, A. (1959). *The Theory of Wing Sections*. New York: Dover Publications, Inc, 2nd edition.
- Birk, L. (2011). NAME 6160–Numerical methods in hydrodynamics. Informal Lecture Notes.
- Hess, J. (1972). *Calculation of potential flow about arbitrary three-dimensional lifting bodies*. Report No. MDC J5679-01, Douglas Aircraft Co., McDonnell Douglas Corporation, Long Beach, CA.
- Hess, J. & Smith, A. (1964). Calculation of non-lifting potential flow about arbitrary three-dimensional bodies. *Journal of Ship Research*, 8(2), 22–44.
- Janson, C.-E. (1997). *Potential flow panel methods for the calculation of free surface flows with lift*. PhD thesis, Department of Naval Architecture and Ocean Engineering, Chalmers University of Technology, Gothenburg, Sweden.
- Katz, J. & Plotkin, A. (2001). *Low-Speed Aerodynamics*. Cambridge, MA: Cambridge University Press, 2nd edition.
- Newman, J. (1986). Distributions of sources and dipoles over a quadrilateral panel. *Journal of Engineering Mathematics*, 20, 113–126.
- Selig, M.S; Lyon, C. . G. P. . N. C. . G. J. (1996). *Summary of Low-Speed Airfoil Data - Volume 2*. Soartech publications, University of Illinois at Urbana-Champaign.

VITA

The Author was born in Cartagena, Colombia. Cartagena is a coastal city located in the northern part of South America. This city is the largest port of Colombia and a very important tourist venue. The author obtained his Bachelor of Science degree in Mechanical Engineering at the Universidad tecnológica de Bolívar, in his home town in March 2004. He worked as a construction engineer in the steel structures construction industry for 2 years. The author also worked for 3 years in the petrochemical industry as a pressure vessel inspector engineer, in a company which is one of the major producers of polypropylene resins worldwide. Motivated by the fact of being watching all kinds of ships from a very early age, and looking to expand his engineering education, the author came to the University of New Orleans to get his masters degree in Engineering, with an emphasis in Naval Architecture and Marine Engineering, in 2009. Once at UNO, the author was given the chance to work as a Research Assistant for Dr. Lothar Birk in the research group of the School of Naval Architecture and Marine Engineering.